CHALMERS
UNIVERSITY OF TECHNOLOGY

Slope stability analysis with FEM

Assessment of the factor of safety by evaluating stress points

Master of Science thesis in the Master's Programme Infrastructure and Environmental Engineering

NATHALI CUOTTO SÁNCHEZ

Department of Civil and Environmental Engineering
Division of Geo-Engineering
CHALMERS UNIVERSITY OF TECHNOLOGY
Gothenburg, Sweden 2015
Master's Thesis 2015:49

MASTER'S THESIS 2015:49

Slope stability analysis with FEM

Assessment of the factor of safety by evaluating stress points

Master of Science thesis in the Master's Programme Infrastructure and Environmental Engineering

NATHALI CUOTTO SÁNCHEZ

Department of Civil and Environmental Engineering
Division of Geo-Engineering
CHALMERS UNIVERSITY OF TECHNOLOGY
Gothenburg, Sweden 2015

Slope stability analysis with FEM
Assessment of the factor of safety by evaluating stress points
Master of Science thesis in the Master's Programme Infrastructure and Environmental Engineering
NATHALI CUOTTO SÁNCHEZ

Examensarbete 2015:49/ Institutionen för bygg-och miljöteknik,
Chalmers Tekniska Högskola 2015:49

Department of Civil and Environmental Engineering
Division of Geo-Engineering
Geotechnical Engineering Research Group
Chalmers University of Technology
SE-412 96 Gothenburg
Sweden
Telephone: +46(0)31-772 1000

Department of Civil and Environmental Engineering
Göteborg, Sweden 2015

Slope stability analysis with FEM
Assessment of the factor of safety by evaluating stress points
Master of Science thesis *in the Master's Programme Infrastructure and Environmental Engineering*

NATHALI CUOTTO SÁNCHEZ

Department of Civil and Environmental Engineering
Division of Geo-Engineering
Chalmers University of Technology

ABSTRACT

The factor of safety is an indication of whether a slope is safe or not, minimum values and other standards are normally stipulated by regional regulations. Traditional slope stability analysis is carried out using limit equilibrium methods, an approach that is easy to get familiar with and relatively simple enough to make calculations. It does, however, present a number of disadvantages, such as assumptions that are essential, primarily regarding the critical slip surface and slices, as the fact that deformations and strains are not considered. Numerical analysis done through finite elements analysis brings a different practice to assessing slopes stability. It is not necessary to make assumptions a priori and it is possible to evaluate stresses and strains generated in the soil, depending on the soil model used. Although this last method has become more extensively used, and the fact that computational tools have become more user-friendly, efficient and faster; there is still limited knowledge on the algorithms and equations used in some commercial programs, and therefore there is a risk of misapplication of these tools. The work here presented deals with the analysis of slopes stability through two different FEM softwares, evaluating the resultant factor of safety by means of comparing the generated stress paths of ten (10) selected stress points along the slip surface. Two cases were examined (total and effective stress based analysis), limited to a single slope geometry and to the Mohr-Coulomb soil model. Alternatives definitions of stability and failure were incorporated by a summary of diverse scientific sources. Similarities, discrepancies, advantages and shortcomings of the programs and the effects on the results were assessed, as well as difficulties regarding the use of one or the other. Caution regarding the simulation under drained conditions is advisable; the effect of pore pressure in the effective stress based analysis presented the most challenges. In general, it was possible to achieve results in very close agreement with both programs, obtaining less than 2% differences for the total stress based analysis and for the effective stress analysis differences were between 2 and 3%. Both are potentially suitable tools to evaluate safety, as long as the user is aware of the limitations of certain soil models and methods for stability analysis.

Keywords: slope stability, factor of safety, finite element methods, soil modeling, Mohr-Coulomb failure criterion, stress paths

ACKNOWLEDGEMENTS

The work presented in this M.Sc. thesis was carried out, during the period of January-June 2015, at the Department of Civil and Environmental Engineering in the Geo-Engineering Division, as part of post-graduate studies at Chalmers University of Technology. This work has been possible thanks to the Swedish Institute Scholarship program that granted me with a scholarship for the period 2013/2015 to conduct my studies in Gothenburg, Sweden.

This master thesis project was carried out in collaboration with Tyréns local office in Gothenburg and it has been a great opportunity to acquire deeper knowledge linked to numerical modelling and Geotechnics; specially it has been an invaluable occasion to grasp how consultancies function and how geotechnical projects are handled in the region.

I would like to express my genuine gratitude to Mats Karlsson, my supervisor at Chalmers University of Technology, for his guidance and sharing valuable knowledge on this subject. I am thankful for his mentorship and motivation to complete this work.

My most sincere thanks to Victoria Svahn, my co-supervisor from Tyréns, for her interesting insights and comments on slopes stability analysis the theory and practice; thanks to the Geotechnics group, for their interest and curiosity about this work.

I would like to thank my friends, old and new ones, for their collective enthusiasm and incentive to take the next step. And, last but not least, I am forever thankful to my family, for being an inspiration and for their unconditional support all along my education and my life.

Gothenburg, June 2015

Nathali Cuotto Sánchez

Content

SYMBOLS AND ABBREVIATIONS

In the following list of the notations and abbreviations used in the report are presented:

c'	cohesion intercept
cu	undrained shear strength
E	Young modulus
FOS	factor of safety
G	shear modulus
g	gravitational constant
Ho	height of slope
I1,I2,I3	full stress invariants
J1,J2,J3	deviatoric stress invariants
K'	bulk modulus
K_0	coefficient of earth pressure at rest
N_0	stability number
p	mean normal stress (σ1+σ2+σ3)/3
p'	mean normal effective stress (σ'1+σ'2+σ'3)/3
q	deviatoric stress
s	mean stress (σ1+σ3)/2
s'	mean effective stress (σ'1+σ'3)/2
t	shear stress (σ1-σ3)/2=(σ'1-σ'3)/2
u	pore pressure
γ	total unit weight of the soil
γ'	effective unit weight of the soil
γw	total unit weight of water
ν	Poisson's ratio
ρ	density
σ1, σ2, σ3	total principal stresses
σ'1, σ'2, σ'3	effective principal stresses
σxx	total Cartesian stress in X direction
σ'xx	effective Cartesian stress in X direction
σyy	total Cartesian stress in Y direction
σ'yy	effective Cartesian stress in Y direction
τ	shear stress
τf	shear strength
τmob	mobilised shear stress
τrel	relative shear stress (from PLAXIS)
ϕ	internal friction angle

ψ	dilatancy angle
CU	consolidated undrained test
ESP	effective stress path
FE	finite element
FEA	finite element analysis
FEM	finite element method
LE	limit equilibrium
LEM	limit equilibrium method
MC	Mohr-Coulomb
SRM	strength reduction method, c/phi reduction method
TSP	total stress path
UU	unconsolidated undrained test

1. INTRODUCTION

The background of this thesis, the aim, goals and objectives are presented in this section. Finally the structure of the report is briefly described.

1.1. Background

A slope can be described as a mass of land with a height difference and an inclination angle respect the horizontal line; slopes can either be man-made or naturally formed. Slope collapse (also referred to as landslides) can cause severe damage to infrastructure, environment and in populated areas, human harm or even human loss.

Soil mass movements can be caused by climate conditions (f. ex. heavy rainfall) or by human activities (f. ex. deep excavations or new heavy constructions). Hence, safety analyses regulate when a slope could become unstable and foresee its possible failure, allowing for corrective actions to be taken on time.

In Scandinavia, landslides are among the main occurring natural hazards, affecting mostly Sweden and Norway (Nadim et al., 2008). Nadim et al., (2008) stresses the concerns of the frequent occurrence of spontaneous landslides in Scandinavia, due to the development of urban areas and human activities close to potential risk areas; and consequently, the importance of taking appropriate measures to prevent accidents.

Several methods have been developed, and are still being refined, with the purpose of generating more accurate and precise examination of slope stability, such as limit equilibrium and more recently numerical analysis methods. The former is known as the classical approach and has been widely employed for a long time. The latter method has been used mainly in research and only more recently in industry. Accordingly, computational tools have been developed to be more efficient, reducing the calculation times required and increasing the amount of data manageable.

Limit equilibrium methods define soil strength by a failure criterion determining a factor of safety when the soil strength is reduced to a minimum state of equilibrium; however, soil deformations cannot be considered during this type of analysis and strength is assumed to be entirely mobilized along some failure zone, therefore separate calculations for serviceability (to evaluate deformations) are required (Nordal, 2011). The use of numerical analysis in geotechnical applications allows for the analysis of both stresses and deformations simultaneously by means of progressive increments of loads until a point of failure is reached or “unlimited deformations “as indicated by Nordal, (2011). Both approaches are based on the strength reduction method (SRM), also known as c/phi reduction, where the shear strength of the soil is gradually reduced.

There is a growing interest from the engineering sector into applying numerical analysis through finite element (FE) software to develop more detailed and economic designs for slope stability. However, numerical analysis are based on complex mathematical theories to reach a result which with the new advances in technology as more accessible softwares, friendlier user-interfaces, and faster computers, specialized

knowledge on FEM is no longer necessary to process soil data. However, there is a risk of running into a “black box” (Nordal, 2011), where users provide in-put data and softwares deliver out-put results without a fair access to equations and algorithms used by the programs, which signifies a risk of geotechnical designs becoming “too mechanical” with little understanding of the calculation processes. Consequently, the idea of understanding better the computational tools available, out-puts generated, and interpreting correctly the outcomes obtained through finite element methods (FEM), results of great relevance when assessing safety analysis and evaluating the right measure to follow.

Hence, the current project analyses the stability of a number of slope cases using FEM softwares. The main focus is to compare the factor of safety (FOS) obtained from two specific software packages; emphasising the influence of the programs used, the stability analysis approach and the failure definition, on the obtained a FOS.

This project is of importance to the geotechnical field to further expand the understanding of the mechanisms behind the numerical analysis approaches of the implemented FE programs. A comparison of different parameters like stress paths of specific selected stress points will be used to evaluate both simulation methods.

1.2. Aim and Objectives

The aim of the project is to evaluate two-cases of slopes, analysing the effect of different numerical analysis approaches on the resulting FOS by means of using two determined FEM programs. The objectives necessary to reach this goal are:

- Define an initial reference (total stress based conditions) case to compare FOS resulting from both FE programs with the classical method of limit equilibrium (LE), using three (3) different softwares SLOPE/W for LE, and PLAXIS and COMSOL for FE. A second case (effective stress based conditions) is defined and evaluated only with FE programs

- Define a factor of safety (FOS) estimation method to be used for the numerical analysis; initially the known strength reduction method (SRM) is used and other alternatives will be brought by scientific sources.

- Define a failure criteria for numerical analysis, indicating if these will affect the final FOS obtained and how. First, non-convergence is used as failure indicator, since this is the common practice.

- Compare both FEM programs and determine if these affect the final result, using stress paths graphs to evaluate similarities between softwares.

1.3. Scope and limitations

The study is expected to cover the use of two specific FEM softwares, PLAXIS and COMSOL-Multiphysics. Results are to be compared with LEM outcomes generated from a known program, SLOPE/W, in an initial reference case.

Verification and validation of data through laboratory testing as well as cost analyses of a project (design, construction, control, etc.) are out of the scope of the current project. Only monotonic loading will be considered; cyclic and dynamic loading will not be reflected on. A single geometry was evaluated.

1.4. Structure of the report

Initially, a literature review on previous investigations comparing numerical analysis methods and programs was completed. As well, a familiarisation with the different LEM and FEM software, SLOPE/W, PLAXIS and COMSOL-Multiphysics respectively, by means of tutorials, exercises or by applying them to known cases were performed.

A stage of gathering needed input data to fabricate the slope cases followed, either by collecting data from real cases or by pre-fabricating study cases.

A reference case (case 1) was studied in an initial stage, using both FE programs and compared to results obtained from LE. After analysing the reference case, a second case was calculated and examined by only comparing FEM programs. A special focus is on comparing the mechanisms of both programs to reach a result; the stress paths generated by programs were used as a tool for this assessment.

The strength reduction method (SRM) was used as a safety analysis method since it is well known and due to its similarity to LEM definition of safety. As a definition of failure, a non-convergence criterion was used on both FEM softwares. However, other criteria for safety analysis and failure definition were studied through scientific papers.

A conclusion regarding the influence of different factors like software, failure definition, FOS definition, soil models and other parameters, on the resulting factor of safety in slope stability analysis is reached and suggestions for expanding a similar investigation is included.

2. LITERATURE STUDY

This section deals with some basic concepts regarding soil stresses, drained conditions, elasticity, plasticity and soil models, including some of the models that will be used later in this thesis report.

2.1. Soils

Soils are an accumulation of minerals in a compact or semi-compact arrangement, generated from the decomposition and weathering of rocks either by physical or chemical processes. Soils are considered to be multi-phased material consisting of a solid phase (grains and minerals), liquid phase (mainly water) and gaseous phase (air and gases), where water and air can be referred to as voids in many cases (Nordal, 2008). Soil grains size and composition are dependent on the transportation and deposition method, it can be either due to wind, gravity, water or glaciers (Knappet, 2012). Being the history of formation and post-deposition highly important to consider when designing and constructing any application in a given soil (Olsson, 2013).

The solid phase of the material, or skeleton of the soil (the soil particles), is responsible for withstanding the stresses to which a soil mass might be subjected to due to loads of any nature. The reaction forces developed at the interparticle contact are thought to resist shear stresses while normal stresses can be resisted by both soil particles and water in voids (in the form of an increase of pore water pressure) (Knappet, 2012). The bearing capacity of soils due to interparticle forces is known as the **principle of effective stresses** presented by Terzaghi (1923,1943) (Knappet, 2012, Nordal, 2008) and it relates total stress (σ), effective stress (σ') and pore pressure (u).

2.1.1. Total and effective stresses

In soil mechanics *total stress* (σ) denotes the total normal forces resisted by soil particles plus the pressure of water in the pores. *Effective stress* (σ') refers to the forces assumed to be transmitted from soil particle to soil particle which can be different in direction and magnitude, having a normal (N') and a tangential (T') component, and therefore *effective stress* (σ') equals approximately the sum of all normal components within an area (Knappet, 2012). The effective stress is expressed as:

$$\sigma' = \sigma - u$$

In soil mechanics, particularly in the case of saturated soils, it is the effective stress that affects all aspects of soils response, the deformability, stiffness, and strength are all dependant on the soil effective stress (Wood, 2009); consequently, it is recommended to express soil models in terms of *effective stresses* (σ'), although it is also possible to express in terms of total stress (Nordal, 2008).

In the case where fluid flow is coupled with soil deformations, due to external loadings, effective stress analysis should account for both processes. Considering soil as laterally confined (only vertical deformations are allowed) and water as an

incompressible material, any increase of total stress (loads) will increase the pressure in the pore water known as **excess pore water pressure.** Since particles can only re-arrange in the vertical direction, and this will occur once the water can flow out of pores, any increase in total stress will mean an increase in the pore water pressure reducing the effective stress, until the excess pore water pressure can be dissipated (Wood, 1990a, Knappet, 2012). The excess pore water pressure and eventual dissipation gives place to two soil conditions referred to as drained and undrained conditions, which are important to determine when doing any reliable and proper soil mechanics analysis.

2.1.2. Drained condition

In order to perform a correct and reliable analysis, the proper conditions of strength parameters and drainage need to be considered. There are basically two main soil conditions under which soil analysis can be approached, either a soil mass is working under *drained* or *undrained* conditions; referring *drainage* to the capacity of soil to dissipate the excess pore water pressure that is generated due to external factors (loading), being time the main variance (Duncan and Wright, 2014). Either one determines parameters required for analysis.

Drained conditions occur when there is no change in pore water pressure when an external load is applied; meaning that additional pore pressure is dissipated through pore water drain. This also indicates that load changes do not create pore pressure changes, since water can flow in or out of soil (there is no stress-induced pressure) (Duncan and Wright, 2014, Knappet, 2012). When this occurs, the soil mass may go through volume changes and the increase in the total stress will be handled by the soil particles (Knappet, 2012).

Drained behaviour should be approached in terms of effective stresses. Different tests can be used to determine the effective strength values. Direct shear test and CU (consolidated undrained) test with pore pressure measurement are fairly commonly used; values from the latter one are thought to be similar as from drained triaxial test (Duncan, 1996).

2.1.3. Undrained condition

Undrained conditions are present when a pore pressure is generated due to an external load applied to the soil, especially in low permeability soils where pore water cannot be drained fast enough. This indicates that changes in external loading will cause a change in the pore water pressure, creating an excess of pore pressure and a reduction of effective stress (Duncan and Wright, 2014, Knappet, 2012).

Undrained behaviour should be studied in terms of total stresses, to avoid using pore pressure values from undrained conditions, that cannot be predicted accurately (Duncan, 1996), or in terms of effective stress with a zero volumetric strain restriction (Nordal, 2008). Strength parameters can be obtained from in situ tests, UU

(unconsolidated undrained) tests or CU together with a normalising procedure according to Duncan, (1996).

2.1.4. Stress path, invariants and deviatoric stress

In order to describe the mechanical behaviour of any solid (including soils), mathematical expressions indicating the *stress:strain* relationship are required, also known as a constitutive model (John B. Watchman et al., 2009, Knappet, 2012). The main variables considered to describe the stress state the in soils response, achieved under a conventional triaxial test, are the mean effective stress *p*' and the general deviator stress *q*, these come into play when developing numerical soil models (Wood, 1990a), expressed as follow:

$$p' = \frac{\sigma'_1 + \sigma'_2 + \sigma'_3}{3}$$

$$q = \sqrt{\frac{(\sigma'_1 - \sigma'_2)^2 + (\sigma'_2 - \sigma'_3)^2 + (\sigma'_3 - \sigma'_1)^2}{2}}$$

The stress paths refer to a series of curves used to better visualise the history of stress and deformation in a soil sample, usually generated from a triaxial test and generally presented in *p':q* graphs (Jamison, 1992). The stress path can be defined as the graphical representation of points, for example in *p'-q* space, indicating progressive changes in the state of stress (Jamison, 1992).

The response of a soil can be described using the mean effective stress *p*' and the general deviator stress *q*, where the mean effective stress *p*' indicates the extent to which all principal stresses are the same while the general stress deviator *q* indicates the extent to which the principal stresses are not the same (Wood, 1990d).

It is worth mentioning that relations (effective and total stresses) defined previously are independent of the choice of coordinate system, however, the components (elements in the matrices) will vary according to the reference systems used (Nordal, 2008); and therefore in a slope the directions of principal stresses components will be affected. Consequently, according to Nordal, (2008), a set of stress variables independent of coordinates systems appears necessary and useful; these are referred to as full stress invariants (I_1, I_2, and I_3) and can be described as:

$$\sigma^3 - I_1\sigma^2 - I_2\sigma - I_3 = 0$$

Where:

$$I_1 = \sigma_{11} + \sigma_{22} + \sigma_{33}$$

$$I_2 = -\sigma_{11}\sigma_{22} - \sigma_{11}\sigma_{33} - \sigma_{22}\sigma_{33} + \sigma_{12}^2 + \sigma_{13}^2\sigma_{23}^2$$

$$I_3 = det(\sigma) = \sigma_{11}(\sigma_{22}\sigma_{33} - \sigma_{23}{}^2) - \sigma_{12}(\sigma_{12}\sigma_{13} - \sigma_{13}\sigma_{23}) - \sigma_{13}(\sigma_{12}\sigma_{23} - \sigma_{13}\sigma_{22})$$

These can also be formulated in terms of principal stresses as:

$$I_1 = \sigma_1 + \sigma_2 + \sigma_3$$

$$I_2 = -\sigma_1\sigma_2 - \sigma_1\sigma_3 - \sigma_2\sigma_3$$

$$I_3 = det(\sigma) = \sigma_1\sigma_2\sigma_3$$

The deviatoric stress invariants (J_1, J_2, and J_3) can also be formulated in terms of principal stresses and in terms of full stress invariants, these are defined as:

$$J_1 = s_1 + s_2 + s_3$$

$$J_2 = -s_1s_2 - s_1s_3 - s_2s_3$$

$$J_3 = det(s) = s_1s_2s_3$$

Where according to Nordal, (2008) *sij* refers to the deviatoric stress matrix, defined as the deviation from the mean stress (defined before), given by:

$$s = \sigma - p$$

These definitions are in terms of total stresses, it is of great importance to keep in mind that in order to base them on effective stresses, pore pressure must be added to the respective expression. These concepts are useful to understand when using numerical analysis approaches to simulate the behaviour of soil.

An alternative representation of stress paths based on Mohr-Coulomb circles are the *s:t* curves, where *s* and *t* are defined as the centre and the radius of the Mohr-Coulomb circle respectively, and these can be seen as the mean shear and the maximum shear stress for plane strain conditions. These are given by:

$$s = \frac{\sigma_1 + \sigma_3}{2}$$

$$t = \frac{\sigma_1 - \sigma_3}{2} = \frac{\sigma'_1 - \sigma'_3}{2}$$

As indicated before, these are represented in total stress terms, to represent them in terms of effective stress terms; pore pressure has to be added only to *s*, since *t* remains the same (Budhu, 2012). It is indicated by Budhu, (2012) that it is necessary to remember that *s:t* curves consider the intermediate principal stress as zero or as a constant value, eventhough in reality it is not. As well, it is indicated how changes in excess pore water pressure (Δu) will be represented differently in *p:q* curves than in *s:t* curves, see Figure 1 (Budhu, 2012).

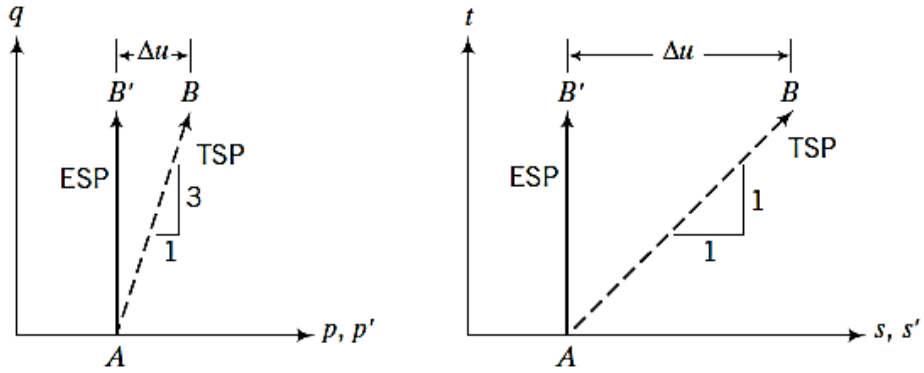

Figure 1. Total and effective stress paths (TSP and ESP respectively) represented in p,p':q and s,s':t curves, (Budhu, 2012)

2.2. Soil modelling

Soil modelling refers to the replication of reality in a simplified way, in order to understand and predict the behaviour of a soil mass under certain conditions. There are different models that account for specific soil parameters, each with a different set of assumptions and simplifications, used to represent one or more particular aspects of soil behaviour depending on the purpose of the study (Budhu, 2012). Since it is only possible to obtain information of a soil mass at discrete locations and therefore many generalisations and assumptions have to be made (Wood, 1990a).

As indicated before the behaviour of a soil is usually described by a *stress:strain* curve from which different parameters can be obtained such as Young modulus (E), Poisson's ratio (v) and shear modulus (G) to describe the stiffness, and shear strength (su or cu) and apparent friction angle (φ) to define strength; these parameters are usually used to determine the response of the material to stress changes (Wood, 1990d). However, the complexity and accuracy of the predictions of soil reaction are highly dependent on the variations of properties in one or more directions. As well, additional aspects such as dilatancy (volume change with shearing) and critical state (unlimited deformations without change in stress or volume) can be missed when far too idealized models are used; therefore soil models should encompass concepts of plasticity and yielding (Wood, 1990a).

2.2.1. Linear Elastic models

Elasticity refers to the property of certain materials where these can recover their initial state after going through deformations due to a certain stress. The isotropic linear elastic model denotes the direct proportionality of shear strain to any shear stress applied, meaning a linear relationship given by Hooke's Law (Knappet, 2012). As indicated before, elastic properties of the soil skeleton are dictated by changes in effective stresses, although elastic behaviour can also be described in terms of total stress (Wood, 1990b). Strain and effective stress are related by, assuming a XY coordinates system:

$$\varepsilon_x = \frac{1}{E}\left(\sigma'_x - v\sigma'_y\right)$$

$$\varepsilon_y = \frac{1}{E}\left(\sigma'_y - v\sigma'_x\right)$$

E and *v* denote the Young modulus and Poisson's ratio respectively. The Young modulus refers to the ration between a stress applied axially and the strain generated in the same direction (Wood, 2009); while the Poisson's ratio in Geomechanics is defined as the ratio of strains in perpendicular directions or the ratio between the horizontal to the vertical strain, in a plane strain analysis (Knappet, 2012).

To define the elastic response, *E* and *v* are sufficient, although in soils mechanics *K* (the bulk modulus) and *G* (the shear modulus) are more common. These last two constants give a reference to a change in volume at a constant shape and a change in shape at constant volume respectively (Wood, 1990b). All four constants are related by:

$$G = \frac{E}{2(1+v)}$$

$$K = \frac{E}{3(1-2v)}$$

Soil behaviour under pure shear is independent of normal stress which means that there is no influence from the pore pressures (water cannot stand any shear) and that *G* will be the same irrespective of the drained condition; on the other hand soil elasticity is dependent on the normal stress and therefore effective stresses as well, meaning that values for drained and undrained conditions differ (Knappet, 2012).

It is worth mentioning that previous definitions apply to isotropic soil elasticity; in reality soils can exhibit either anisotropic elasticity (different in different directions) or non-linear elasticity. However, isotropic linear elasticity is used to define the stress path for appropriate laboratory testing and to estimate deformations of geotechnical structures (Wood, 1990b). Non-linear models have been used for their easy implementation in FEM and simplicity; however due to shortcomings of the non-linear model, especially near failure, elastic-plastic models are more used (Nordal, 2008).

2.2.2. Elastic-perfectly plastic model

The irrecoverable and permanent deformations a material undergoes after the loads have been removed are known as plastic deformations. Elastic-plastic model refers to a combination of elastic behaviour and plastic behaviour of a material, see Figure 2, under which the total strains are the sum of elastic plus plastic strains where all strains under the failure line are considered elastic (following Hooke's Law) and plastic above this line (Nordal, 2011).

Plastic models allow determining failure and critical states, to get an idea of irrecoverable strains and to simulate changes created in the material behaviour due to plastic strains (Karstunen, 2014a).

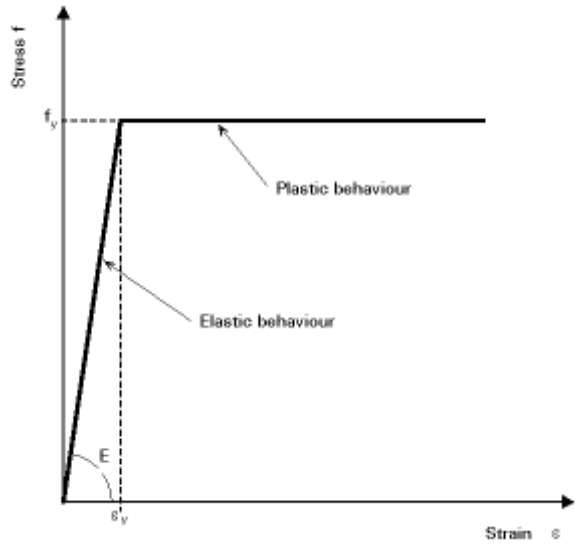

Figure 2. Idealised linear elastic-perfectly plastic stress:strain graph, (Slovenian, 2010)

Yield criterion refers to the limit between elastic and plastic deformations. For cases in one dimension, it is represented by a point, while in a two-dimension case *yielding* occurs when the stresses approach a curve or a surface in 3-dimension cases; in general yielding is associated to a change in the stiffness response of a material (Wood, 1990c). When perfectly plasticity model is being used the yield surface remains constant. The yield surface is usually express in terms of stress invariants, commonly *p':q* curves (Karstunen, 2014a). The direction of the plastic strain increment is given by the flow rule which defines the mode of deformation (Nordal, 2008).

Among the elastic-perfectly plastic models used to define *yield criterion* in Geotechnics, the most commonly known are the models proposed by Tresca (1864) and Von Mises (1913) which can be appropriate for undrained saturated soft soils; although none of these models include a function of the mean stress (Yu, 2006).

The Tresca model proposes that yielding occurs when a *maximum shear* stress reaches a shear strength limit (Su), where *Su* is the undrained shear strength; for computational purposes it is often expressed as a function of the second invariant of the deviatoric stress, J_2, (Yu, 2006). Von Mises, on the other hand, proposed that yielding occurred when the second invariant of the deviatoric stress (J_2), reaches a critical value that equals the radius of the yield surface in the π-plane, representing the undrained shear strength in pure shear (Yu, 2006). However, both models present certain singularities that may represent mathematical inconvenients; as well none is consider to be adequate for cohesive-frictional material, unlike the Mohr-Coulomb model where yield is a function of the first invariant or mean stress and therefore more suitable for frictional material (Yu, 2006).

The Mohr-Coulomb defines the stress state of an element in terms of shear stress (τ) and normal effective stress (σ'). Yielding (failure) under the Mohr-Coulomb criterion occurs when the mobilised shear stress (τ_m) is equal to the shear strength (τ_f) of any soil mass. Then the failure envelope is approximated to a linear relationship defined by:

$$|\tau| = c' + \sigma'_n tan\phi = \tau_m = \tau_f$$

Where the strength parameters are given by ϕ as the internal friction angle (or angle of shearing resistance) and c' as the cohesion intercept with the vertical axis, also referred to as cohesion, see Figure 3 (Knappet, 2012).

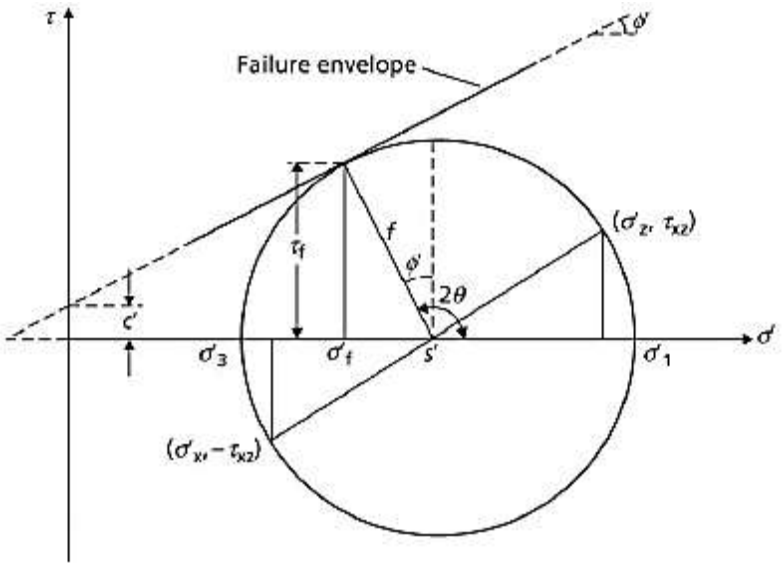

Figure 3. Mohr-Coulomb failure criterion, (Karstunen, 2014a)

For principal effective stresses $\sigma'_1 \geq \sigma'_2 \geq \sigma'_3$, the yield criterion can also be written as:

$$(\sigma'_1 - \sigma'_3) = (\sigma'_1 + \sigma'_3)sin\phi + 2c\ cos\phi$$

This expression can similarly be written in terms of principal total stress, and the representation of the Mohr circles will have the same diameter but separated by the value of pore pressure (u) (Knappet, 2012). Alternative ways of representing the Mohr-Coulomb criteria is using either a *p':q* curve (effective mean stress: deviatoric stress) or *s':t* curve (representing the position of the centre of a circle and the radius respectively) , these are appropriate for certain plane strain situations (Nordal, 2011).

It is necessary to keep in mind that Mohr-Coulomb is a model with simplifications and assumptions; therefore there are some shortcomings of using this model. Specially related to flow rule (associated or non-associated) it considers continuous dilation angle when shearing, it cannot account for volume change while shearing and it overestimates shear strength under undrained conditions in soft soils (Karstunen, 2014b).

The analysis and study of the cases analysed in this report will be based on the Mohr-Coulomb failure criterion, stress paths generated from the different computational tools will be presented in terms of *s':t* curves.

3. SLOPE STABILITY ANALYSIS

This section deals with some of the basic concepts regarding slopes stability, limit equilibrium (LEM) and finite element methods (FEM); including different scientific papers and investigations sources where alternatives definitions of stability and failure have been proposed.

Slopes are unsupported soil masses formed either by human activity (excavations or embankments) or by natural processes (erosion or deposition); due to external factors these can become unstable and collapse; gravitational and seepage forces seem to be the most frequent causes of instability (Knappet, 2012).

To prevent a slope from reaching failure and collapsing, a safety analysis based on the ultimate limit state (ULS) is required; this is conventionally done by using LEM together with a series of factoring of the loads and the strength of soil (Nordal, 2011). Alternatively, FEM are being incorporated to the analysis of serviceability limit states (SLS), meaning to estimate deformation of the material, however this tool is still not so widely used to assess the stability of slopes.

3.1. Limit Equilibrium methods (LEM)

Limit equilibrium method idealises a sliding soil mass as divided into several slices where each slice is analysed (supporting and reacting forces) as a single unit and later added together with the rest of slices, see Figure 4. Various assumptions, mainly on the slip surface and inter-slice forces, are then essential to be made to initially calculate the slope safety.

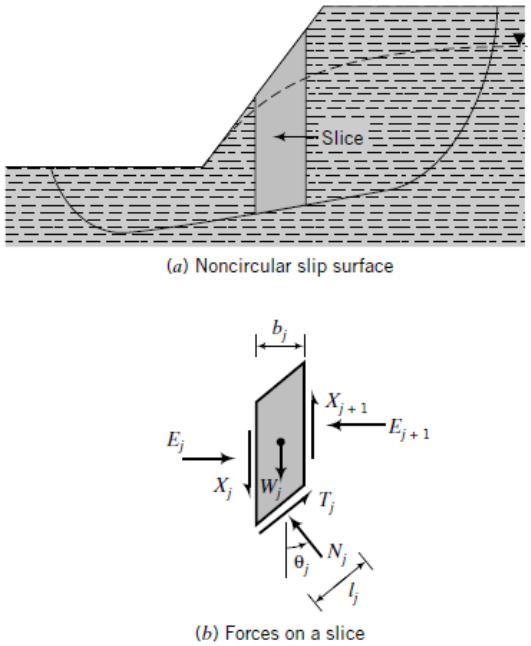

Figure 4. Example of a slip surface and a slice, indicating slice's forces and dimensions assumed,(Budhu, 2012)

There are several different methods developed under the slices theory, where the main differences lay in the assumptions made by each author on the inter-slice forces and shape of slip surface (Griffiths and Lane, 1999). A small summary of the main differences of each method, the author and assumptions are shown in Figure 5.

Method	Assumption	Failure surface	Equilibrium equation satisfied	Solution by
Swedish method (Fellenius, 1927)	Resultant of interslice force is zero; $J_s = 0$	Circular	Moment	Calculator
Bishop's simplified method (Bishop, 1955)	E_i and E_{i+1} are collinear; $X_i - X_{i-1} = 0$, $J_s = 0$	Circular	Moment	Calculator
Bishop's method (Bishop, 1955)	E_i and E_{i+1} are collinear; $J_s = 0$	Circular	Moment	Calculator/computer
Morgenstern and Price (1965)	Relationship between E and X of the form $X = \lambda f(x)E$; $f(x)$ is a function = 1, λ is a scale factor, $J_s = 0$	Any shape	All	Computer
Spencer (1967)	Interslice forces are parallel; $J_s = 0$	Any shape	All	Computer
Bell's method (Bell, 1968)	Assumed normal stress distribution along failure surface; $J_s = 0$	Any shape	All	Computer
Janbu (1973)	$X_i - X_{i-1}$ replaced by a correction factor, f_0; $J_s = 0$	Noncircular	Horizontal forces	Calculator
Sarma (1975)	Assumed distribution of vertical interslice forces; $J_s = 0$	Any shape	All	Computer

Figure 5. Different assumptions of different methods of slices for slope stability analysis based on LEM, extract from (Budhu, 2012).

For example, using a single method two different slip surfaces, out of the many evaluated, were assumed and calculated, as part of the LEM theory, in order to determine which is the most critical. In a closer look to the forces assumed in a specific slice taken from the slope under study, it can be seen in Figure 6, that 1) for each different presumed slip surface, the same slice will differ slightly in shape and the acting forces , 2) forces do not always agree in the end-start point, as shown in Figure 6.

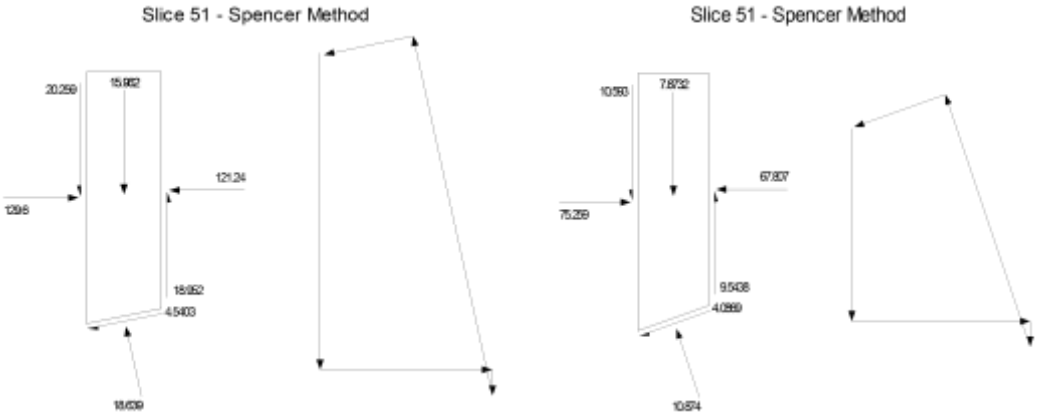

Figure 6. Same slice number for two different assumed slip surfaces under the same method for a same slope case, indicating differences between both.

In general, all the methods developed under the LEM approach define FOS (factor of safety) according to the strength reduction method (SRM), under which the value is found when a state of barely equilibrium is established (Duncan, 1996).

One of the main advantages of these methods is that hand calculations can be done with most of the different methods (Krahn et al., 2004). As well, the concepts are not difficult to understand and the techniques can be applied using simpler computational tools, such as a programmed spread sheets.

On the shortcoming of these methods, no information on the strains in the slope nor how these vary along the slip surface is available (Duncan, 1996, Nordal, 2008). Some authors also indicate the possibility of the inter-slices shear and normal forces may violate the Mohr-Coulomb criterion, since this criterion is not considered along the vertical interface between slices (Y . M . Cheng and Lau, 2014).

However the limitations of LEM procedures, these are still of use for slope analysis as long as the uncertainties involved are considered and taken into account while designing (Duncan, 1996).

SLOPE/W is a computational tool used to study mainly the stability of different slopes applying the theory of LEM. This computational tool is to be used as a comparison of the initial case (or reference case) with the FOS obtained using FEM programs.

3.2. Finite Element methods (FEM)

Finite element methods are founded on two basic concepts, first a continuum is formed by a specific number of smaller, simpler elements joined at nodes and with a limited number of degrees of freedom (DOFs), determined by the number of nodes per element and the number of degrees of freedom per node. Second, the differential equations are solved by the application of numerical integral methods (Ashcroft and Mubashar, 2011). These differential equations in a simpler form can be solved through matrix methods. Ashcroft and Mubashar, (2011) indicates that FEM is still a technique to simulate reality, and therefore some errors can be encountered.

In Geomechanics, the application of FEM is done similarly as to structural mechanics, by means of the *displacement method*. This method refers to the study of displacements of the nodes due to applied forces or loads to a structural body or (in this case) a soil (Nordal, 2011).

An approximate solution of the entire soil volume is obtained by adding together the behaviour of each element. The performance of every element is analysed by means of *shape functions*, often denoted by *N*; these are usually in simple polynomial form (of different orders) and it is required as many *shape functions* as number of nodes there are in an element (Karstunen, 2014b).

In the analysis of slope stability, non-linear FE methods offer great advantages over conventional methods as indicated by Griffiths and Lane, (1999). It is not only more accurate and graphical friendly for routine calculations, but also reduces the possibility of misleading results by the use of conventional “slip circle” calculations.

In comparison with LEM, using FEM no assumptions regarding shape and location of failure surface is required (Griffiths and Lane, 1999), as well as no further studies on slides side forces are needed. Among the FEM out-puts, deformation at working stress

levels is available and progressive failure can be monitored, including shear failure (Griffiths and Lane, 1999).

Modelling can be done in one, two or three dimensions, depending on the requirements of the analysis. Two dimensional (2D) simulations can be considered as “plain strain” or “axisymmetric”, with only two translational degrees of freedom per node. The first model assumes a relative uniform cross section where displacements and strains in the perpendicular direction are much smaller (can be disregarded) and normal stresses are taken into account. The second model is usually used for structures with uniform radial cross section and loading occurs through the central axis, where deformations and strains are assumed to be equal in any radial direction (Brinkgreve et al., 2014a).

The FEM consists of three stages pre-processing, processing and post processing as indicated by Ashcroft and Mubashar, (2011). In the pre-processing stage, the model is created with all the input data available. At this stage geometry is defined as well as material properties, type of analysis, loads, boundary conditions and mesh element type and size; it is necessary to have a clear understanding of what is required from the analysis and what input is needed to complete it (Ashcroft and Mubashar, 2011). The mesh generation has become more commonly set by default by commercial software. Nonetheless, this can be defined by the users as long as a proper understanding of the mesh density and change in specific direction, geometric types of elements, number of nodes per element and the elements connectivity (DOFs of common nodes), is accomplished. The generation of the mesh and later refinement are relevant for the efficiency and reliability of the analysis (Ashcroft and Mubashar, 2011).

The following two stages, processing and post processing refer to the actual solving and later analysis of results. For users, the most relevant stage is the post processing where errors can be detected and fixed, refinement of mesh can be decided, and answers to the initial questions can be provided in a further analysis of results (Ashcroft and Mubashar, 2011).

For the following project two different programs will be used, PLAXIS and COMSOL-Multi-physics. Although both programs are used for FEM analysis, there are some differences especially in the user interface, model building such as step-by-step used, solvers available, mesh generation, etc. Some of the most relevant features of both programs will be further explained in the following sections.

Given a typical slope geometry where deformation and stresses are more significant in transversal section than in the longitudinal; it is assumed, for the purposes of this work, to proceed with slope stability analysis in a plane strain model.

PLAXIS 2D

PLAXIS 2D is a finite element program used for the simulation and analysis of deformation and stability of different geotechnical applications, including a wide range of soil constitutive models considering non-linearity, anisotropy and time-dependant behaviour of soils (Brinkgreve et al., 2014b). In this report it was used *PLAXIS 2D version AE (Build 4217).*

The Mohr-Coulomb model is widely known and the most commonly used for certain soil conditions; in combination with the SRM, it is possible to perform a stability analysis for slopes. There are also other advanced models available, as well as the user-defined soil model option, if desired (Brinkgreve et al., 2014b).

In PLAXIS 2D as any other program, it is necessary to initially define the geometry, soil parameters, water level and other initial available data. Once the soil stratigraphy (layers) is defined, the structural elements such as loads and the boundary conditions (BC) are added. The next step is to generate a mesh that can be done with different mesh automatic refinement options; however only triangular elements are available with the possibility of choosing only between two (2) discretisation options (6-nodes or 15-nodes). The water level and flow conditions can be reviewed once again in the "Water" tab. Finally the calculation procedure is specified by the user under the "Construction stages" tab (Brinkgreve et al., 2014a).

It is indicated in the reference manual that compressive stresses and forces are taken as negative, while tensile stresses and forces are considered positive, as part of the sign convention used (Brinkgreve et al., 2014a). It is also necessary to mention the considerations of the program on the principal major and minor effective stresses; being σ'_1 the largest compressive principal stress (major principal stress) and σ'_3 the smallest compressive principal stress (minor principal stress) (Brinkgreve et al., 2014a).

$$\sigma'_3 \geq \sigma'_2 \geq \sigma'_1$$

Results of stability analysis are highly sensitive to mesh size and the number of nodes per element. The program automatically generates the mesh, where users can choose to locally or globally refine the generated mesh (Brinkgreve et al., 2014b). For 2D simulations there are two options for discretisation of the element, by quadratic functions (2^{nd} order and 6-nodes elements) and quartic functions (4^{th} order 15-nodes elements). The greater the number of nodes per element the more accurate the results obtained but also the longer computational time is required (Brinkgreve et al., 2014b).

There are a number of predefined soil models available for the user to choose from. Soils conditions and parameters can also be modified; a user defined option is also available. In order to include the material characteristics and properties in the model, it is possible to add them from either user's data available or simulating conventional soil tests such as oedometer and triaxial tests.

In the Mohr-Coulomb model, it is possible to express the effective stress state in terms of effective strength parameters (ϕ' and c'), and for undrained cases, the internal

friction angle can be set to zero (0) and set the value of undrained shear strength (Cu). In order to make undrained analysis, there three available options in PLAXIS namely *UNDRAINED (A), UNDRAINED (B)* and *UNDRAINED (C)*, referring to analyses with effective strength parameters, with total strength parameters (or undrained strength) and effective stiffness parameters, and with effective strength and stiffness parameters respectively (Brinkgreve et al., 2014c).

For the Mohr-Coulomb model, a higher value of the Poisson's ratio is recommended by Brinkgreve et al., (2014). When the Mohr-Coulomb model is used for gravity loading the following expression for *Ko* is thought to give more realistic values:

$$K_0 = \frac{\sigma'_h}{\sigma'_v} = \frac{\upsilon}{(1-\upsilon)}$$

It is possible to display results in different ways, either charts can be generated for single pre-selected nodes points or post-selected (or stress points) after running the simulation, or by graphical interactive displays of resulting data in the entire geometry analysed.

For the current analysis, only 15-noded elements were used, and different mesh densities were studied to understand the impact of the size of the mesh in the results. As well, the linear perfectly-plastic Mohr-Coulomb model, available in the software, was used. It is indicated that for this model a constant average stiffness is assessed which results in reduced computational time (faster results) (Brinkgreve et al., 2014c). On the downside, Mohr-Coulomb model includes a limited number of soil features, it does not take stress, strain, nor stress paths-dependency of the soil stiffness nor anisotropic stiffness of soil (Brinkgreve et al., 2014c). Anisotropy, however, was left out of the scope of the present work. This thesis considered *UNDRAINED (B)*, for the total stress based case analysis (case 1), and *DRAINED* for the effective stress based analysis.

COMSOL Multi-physics

Multi-physics modelling refers to the use of FEM to study the coupling of different physical processes such as thermo-structural, fluid-chemical, electro-thermal, fluid-structural, etc. Through this coupling, it is possible to further analyse the effect of one process in the response to the other process and vice versa (Ashcroft and Mubashar, 2011). For purposes of this work *COMSOL v 5.0* was used.

To simulate and analyse stability in soils/rocks undergoing certain processes, COMSOL Multi-physics recently developed a module named "Geomechanics Module" as part of the physics group "Structural Mechanics Module" which is designed for stresses and strains study in solids. Using this module, it is possible to simulate applications such as deep excavations, retaining structures, tunnels, slope stability and many others. As part of the program, some known mathematical soil models are available and can be used by default or modified to a user-defined requirements for a specific cases (COMSOL Multi-physics, 2015).

As part of the signs conventions, tensile stresses and strains are considered to be positive, where σ'_3 is the major principal compression stress; the principal stresses are dictated by:

$$\sigma'_1 \geq \sigma'_2 \geq \sigma'_3$$

The modelling procedure in COMSOL is done following what is known as **Model Builder**, which as indicated in the documentation *"it is a model tree with all the functionality and operation for building and solving models and displaying results"* (Multi-physics, 2015). This is divided into branches which are divided into nodes, each with settings and properties that can be accessed and modified to fit the needs of the user.

In COMSOL analysis are evaluated by components where different space dimensions are available, 1-D, 2-D or 3-D; as well as between either an axisymmetric analysis component or not.

There are several options to define the wanted geometry; it is possible to create a set of lines, primitive figures (triangles, squares, etc.), polygons, or it is also possible to edit a solid (by extrude, sweep, etc.) to the wanted shape. Importing geometries from CAD documents is also possible.

The mesh can be either user-controlled or physics-controlled, where the user can select the type of element, the maximum and minimun size. Different types of elements can be selected, as well as the discretisation shape order can be chosen from linear (1^{st}-order element) to quintic (5^{th}-order element) which has to be designated for each physics added.

Soil plasticity can be simulated either by the available models within the program or create user-defined yield functions. Material properties can be defined under the corresponding "physics" or as a general definition under the node "material" (COMSOL Multi-physics, 2015).

In order to monitor and evaluate the development of a variable from a time-dependant, frequency-domain or parametric simulation, COMSOL counts with a tool refer to as *probes.* There are different types of probes available depending on the type of assessment the user requires (Multi-physics, 2015). In this work, *domain point probes* were used to obtain the value of stresses generated at specific points during the study.

As part of the setting of a *domain point probe*, the user can specify the *frame* to work with and respective coordinates. The different *frames* available in COMSOL are spatial, material, geometry and mesh-frame. These define different coordinates systems depending on the convenience to interpret equations in the Eulerian or Lagrangian formulations (Multi-physics, 2015). For purposes of the studied cases, *domain point probes* were studied under spatial-frame, although as indicated in COMSOL-documentation, since geometric non-linearity was not studied, frames are thought to be referenced to the same coordinates system in spite of the frame selected.

Solution methods in this program can be either of a direct or an iterative type. The first method refers to finding an approximation of the solution by matrix decomposition

into a number of operations depending on the number of unknowns. The latter one approaches the solution by an initial guess and a future improvement of result by a number of iterations (Marra, 2013).

The direct solvers available in COMSOL are MUMPS (Multifrontal Massively Parallel Sparse direct Solver), PARDISO (Parallel Direct Sparse Solver Interface), and SPOOLES (Sparse Object Oriented Linear Equations Solver). All of which use LU Decomposition (lower upper triangular matrix) as a matrix factorisation method (Frei, 2013). Being speed the main relevant difference, from PARDISO as the fastest to SPOOLES the slower but requiring less memory (Frei, 2013).

Iterative solvers, unlike direct solvers, reach a solution progressively and not in one computational step, with the possibility of observing the gradual reduction of the error while approximating to a solution. Available solvers in COMSOL are GMRES (Generalized Minimal Residual Method), FGMRES (Flexible Generalized Minimal Residual Method), BicGStab (Biconjugate Gradient Stabilized Method), and CGS (Conjugate Gradient Square Method). These solvers require significantly less memory usage for the same problem than direct solvers. However, different adjustments depending on the nature of the constitutive equations to be solved are necessary (Frei, 2013).

In a similar style to PLAXIS, in COMSOL it is possible to generate charts, graphs, tables, animated outputs and different displays of information. Data can as well be exported and handled for example in excel sheets depending on the requirements of the users.

In order to replicate as closely as possible the modelling in both programs, the features used in PLAXIS were reproduced as well in COMSOL. For both cases studied, a 2-D plane strain analysis was performed and polygons were used to create the slope geometry. Each physics used, for the cases analysed in this report were discretised with quartic triangular elements with 15-nodes, and the mesh was tailored under user-controlled option to ensure as many similartities to PLAXIS as possible. For additional analysis of stresses generated in specific stress points, *domain probe points* were used. Soil properties (or materials) were created within the *Linear-Elastic* and *Soil Plasticity* sub-branch (or node).

For the thesis purposes only direct solver MUMPS was used together with a parametric sweep of the FOS parameter from 1 until non-convergence was reached; step size was adjusted depending on the study. As for the non-linear method of calculation, “double dogleg” was used with case-dependant adjusted tolerance and damping factors.

From the information obtained for each *domain probe point,* graphs were generated and data exported to excel, as well as data from PLAXIS, in order to compare them.

4. SAFETY ANALYSIS IN SLOPES

The definition of safety and the methods used to analyse slopes stability will be presented next; this will be followed by the currently used definition of failure and some alternatives proposed by different authors.

4.1. Definition of factor of safety (FOS)

In order to assess the stability of a natural or man-made slope, a FOS must be determined (Khosravi and Khabbazian, 2012). In the classical LEM theories, the factor of safety is defined as "*the ultimate shear strength divided by the mobilised shear stress"* (Cheng and Lau, 2014) together with the assumption that this rate is constant along the entire slip surface. In many cases, a minimum value of this factor is targeted as an indicator of stability, depending on the construction stage or uncertainty level (Duncan, 1996).

For the case of FE analysis, there are two main procedures that have been used in the slope stability analysis; that is the gravity induced (overloading) method and the strength reduction method (Khosravi and Khabbazian, 2012). The gravity induced method defines the factor of safety as the ratio of the total resisting forces to the total driving forces along the slip line. While in the strength reduction method, the factor of safety is defined as the factor by which the shear strength of the soil is to be reduced to reach a state of critical equilibrium (Khosravi and Khabbazian, 2012).

4.1.1. Strength Reduction Method (SRM)

The SRM concept is based on the progressive reduction of the shear strength of the soil by a specific factor until the minimum shear strength, to keep a narrowly state of equilibrium, is reached (Duncan, 1996). The SRM is the most commonly used in FEM analysis, given its similarity with the classical definition used in LEM (Brinkgreve and Bakker, 1991, Khosravi and Khabbazian, 2012).

The SRM factor of safety is defined then as:

$$FOS = \frac{S}{S_c} = \frac{c + \sigma' * \tan(\phi)}{c_c + \sigma' * \tan(\phi)_c}$$

Where S refers to the shear strength according to the Mohr-Coulomb failure criteria, c is effective cohesion, ϕ is the effective friction angle and σ' is effective stress (Brinkgreve and Bakker, 1991). And, the subscript $_c$ indicates the critical parameters needed to ensure a barely state of equilibrium (Brinkgreve and Bakker, 1991).

The SRM is being adopted more increasingly by commercial geotechnical software with FEM (Cheng et al., 2007). Cheng et al., (2007) and Griffiths and Lane, (1999) enlisted some of the more evident advantages of the method in comparison with limit equilibrium theory, such as: (i) the critical failure zone is automatically found, no assumptions are made a priory, (ii) since no slices are assumed, there is no need to anticipate information on the inter-slice shear force distribution, (iii) difficult and

complex geometries can be simulated obtaining information on stresses, strains, movements, among other (Cheng et al., 2007, Griffiths and Lane, 1999).

However, Xu et al., (2011) indicates the lack of a standard unification on how the method is adopted is a great disadvantage of this technique. Among other shortcomings, choosing the appropriate constitutive model, the correct boundary conditions and the effect of the chosen failure condition/failure surface affect the effectiveness of the technique (Cheng et al., 2007).

Cheng et al., (2007) also indicates that for SRM a unique failure surface results from the analysis, and an alternative failure surface cannot be easily determined; even more, a case where a more severe global failure surface was not detected with this technique while a less relevant local failure surface was the one generated with SRM was analysed by Cheng et al., (2007). As well, remarks on the sensitivity of the technique to nonlinear solutions algorithms/flow rule for some cases, i.e. slopes with a soft band, were concluded after a study case indicating the mesh dependency of the case. On the mesh dependency, it is noted that only minor noticeable differences were found between square and distorted elements, however, in cases of small strength parameters, *c', φ',* or the case of soft bands problems arise with SRM (Cheng et al., 2007).

4.1.2. Gravity loading (overloading) Method

The gravity loading technique has been recently defined and used as alternative indicator of stability; this differs somewhat from SRM. This method relates the total resisting forces to the total driving forces along a certain slip line (Khosravi and Khabbazian, 2012). Under this method the gravity acceleration is gradually increased (the materials density) and applied to the entire model until the capacity of the slope reaches its limit state (or fails) while the strength parameter given by the cohesion intercept (*c'*) is kept constant (Xu et al., 2011). Where the effect of the gravity is reflected directly in effective stress (σ') and can be estimated by:

$$\tau = c + \frac{\sigma' * \tan(\varphi)}{Fi}$$

The factor of safety of the slope can be described as the ratio of the gravitational acceleration at failure compared to the actual gravitational acceleration (Khosravi and Khabbazian, 2012), and the expression is as the following:

$$F = \frac{g'}{g}$$

Where *g'* refers to the current gravity acceleration, which can be determined from soil parameters of the initial state of the soil. And *g* refers to the gravity acceleration, which will be progressively increased until the slope reaches a failure state. It is worth noting that since the deadweight is increased, so is σ and τ.

There are some downsides regarding this method, and it is mainly due to the inaccuracy when analysing gentle slopes and large friction angles (Xu et al., 2011).

4.2. Definition of failure

The physical failure of a soil slope, or the collapse, might be caused by different external and internal factors, such as new constructions, earthquakes, intense rainfall, erosion, soil type, stratification of soil, slope geometry and groundwater conditions, just to enlist some (Budhu, 2012). Depending on the soil texture, slopes collapse can be as translational slide occurring commonly in coarse-grained material and rotational slide common in fine-grained soils. The rotational slides can be sub-divided as base slide, toe slide and slope slide (Budhu, 2012) and these are indicated in Figure 7.

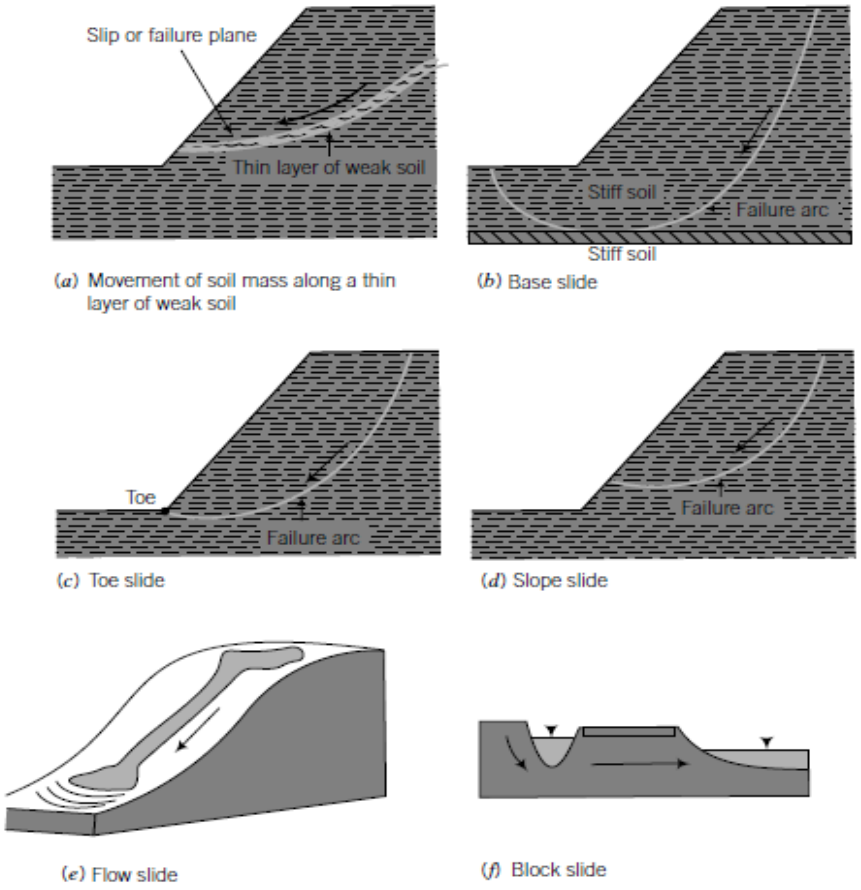

Figure 7. Common soil slopes slides,(Budhu, 2012)

However, representing the reality of each case results too complex, time consuming and difficult considering all single parameters and specific features of every slope. Therefore, different techniques have been developed simplifying the cases to reach a result in an acceptable time frame and simple enough to consider all needed constraints. Failure definitions used in both LEM and FEM procedures are idealisations of when collapse in a slope is expected to occur. Consequently, there is no single, universal definition and these can be case and user dependent.

In finite element analysis, modelling of failure is a concept in constant development and revision. According to Ashcroft and Mubashar, (2011), one of the simplest models

to simulate failure is based on plastic yielding, where a "limit state" is reached by progressive yielding of the element.

The instability of a slope, or limit state, is not clearly and strictly defined and it can be reduced to three different criteria based on SRM (i) non-convergence of the solution, (ii) extension of the plastic zone from toe to the top of the slope or equivalent shear strain (or plastic strain) along the potential slip surface, and (iii) rapid increase in nodal displacement on the slope surface (Khosravi and Khabbazian, 2012, Xu et al., 2011, Nian et al., 2011).

4.2.1. Non-convergence

Based on SRM definition, it is assumed that a state of failure is reached when the factor of safety obtained is below 1.0, and a solution cannot converge (Chen et al., 2011). A slope reaches the limit state (failure) when no stress distribution can be found to fulfil both the failure criterion and global equilibrium, this is achieved by setting iterative criterion where if non-convergence occurs within a maximum number of user-specified iterations failure has been reached (Nian et al., 2011).

Iterative non-convergence is usually recommended because it is ready to code and operate in practice and it can generate the factor of safety and failure surface (Nian et al., 2011).

4.2.2. Extension of the plastic zone from the toe to top

Non-convergence method does not necessarily indicate collapse; therefore some authors have used an alternative criterion to define failure based on the distribution of the plastic zones. The failure is recognised to occur when the plastic zones (enclosing the critical slip lines) are interconnected and pass through the slope from the toe to the top (Zheng et al., 2005, Zheng et al., 2009). The critical slip surface in the plastic zone is as Zheng et al., (2009) pointed out formed by "points where the equivalent plastic strain takes the local maximum in the vertical direction"; that is that the critical slip line (failure surface) goes through the points of maximum plastic strain from a series of vertical lines (Zheng et al., 2009).

Zheng et al., (2005) also mentions that a visualization technique is required to verify that these plastics zones are connected and to verify where they go through. It is recommended to draw the contour lines of the generalized plastic stain (GPS) to indicate the plastic zones. A definition of GPS, designated as ε_p, is shown in the following expression:

$$\varepsilon_p = \int d\varepsilon_p = \int \left[\frac{2}{3}\left(d\varepsilon_p\right)^T\left(d\varepsilon_p\right)\right]^{1/2}$$

It is indicated by Zheng et al., (2005) that in case of a slope reaching the critical state, a contour line of GPS with a very low value (marginally over zero) will be generated. It is declared that the failure degree can be illustrated more clearly, as the larger the value

of GPS the larger the deformation the domain has experienced (Zheng et al., 2005). An example of the graphic representation can be seen in Figure 8.

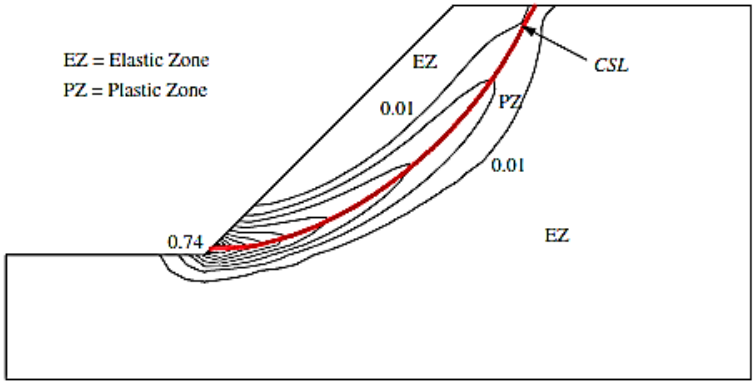

Figure 8. Critical slip lines (CSL) and generalised plastic strain (GPS) from case studied by (Zheng et al., 2005)

It is recommended a re-adjustment of the Poisson's ratio to satisfy the *φ-v* inequality in order to avoid the overestimation of the plastic zones and reduce the calculation times (Zheng et al., 2005). In this research it was shown that if this inequality is not fulfilled and the non-convergence criterion is used, there is the possibility of that the analysis will not converge within the user-specified iterations and therefore the FOS might be underestimated.

4.2.3. Nodal displacement on the slope surface

Some authors also indicate that a maximum displacement can be found to be a better definition of failure compared to the non-convergence criterion. Khosravi and Khabbazian, (2012) define more clearly this criterion with a graph where it is evident the point where horizontal displacements at a specific node start increasing drastically, see Figure 9. Although in comparison with the full extension of the plastic zones from toe to top of the slope, it does not always visually evident the slope collapse (Khosravi and Khabbazian, 2012).

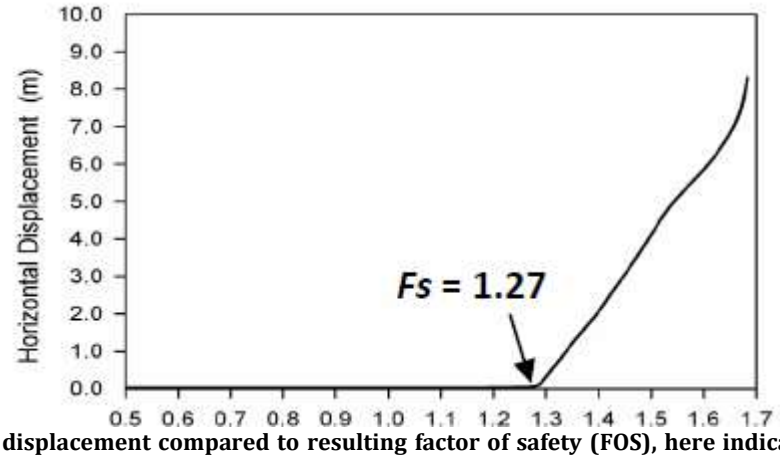

Figure 9. Nodal displacement compared to resulting factor of safety (FOS), here indicated as FS, from case studied by(Khosravi and Khabbazian, 2012)

5. METHODOLOGY FOR OBTAINING FOS

The approach used to define and analyse different slope cases will be presented in the following section, including the different assumptions and simplifications used.

5.1. General procedure and assumptions

The geometry of the slope was decided to be a horizontal distance of twice the height of slope (Ho) in both directions and also to the bottom layer, as measure to avoid interference with boundaries. Both the chosen geometry used in both cases and the water table are shown in Figure 10. This geometry was found to be regularly used by different authors from the literature survey done, where commonly a slope of 2:1 (Horizontal: Vertical) was used and evaluated (Griffiths and Lane, 1999,Glamen and Nordal, 2005, Glamen et al., 2004), such as the one defined below.

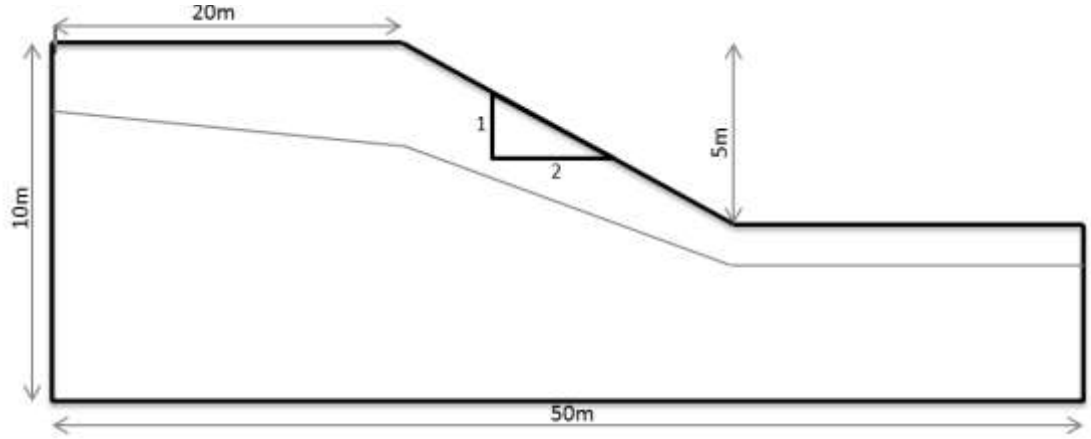

Figure 10. Geometry of both analysed cases. In case 1 no water table is considered.

As part of establishing the initial soil parameters, a rough back-calculation was performed using Taylor's graphical method, obtaining a minimum value for the shear strength for a specific unit weight and for the proposed geometry (Budhu, 2012). Taylor's method is given by the following expression:

$$FOS = N_o \frac{\sum(s_u)_f}{\sum(\gamma z)_f}$$

Where *No* is stability number which is dependent on the slope geometry, FOS is the factor of safety which was set to the required minimum of 1.5, γ is the unit weight set to 16[kN/m^3] and Z the height of the slope (Ho) set to 5 [m] (Budhu, 2012). Therefore by means of using the respective method's charts, the minimum undrained shear strength (cu or su) was obtained.

Then for study case 1, total stress based analysis, it was assumed a homogeneous layer with constant shear strength (cu) upto certain depth, after which the shear strength increases per meter of depth.

For the case 2, effective stress based analysis; the drained shear strength was initially set to a 10% of the undrained shear strength (cu). Later, the same case was modelled

using a higher value of drained shear strength (50% of cu), the reasons for this will be explained later on. The rest of the strength and stiffness parameters are indicated in Table 1 and are estimated to be related to some common soft soil characteristics in the west region of Sweden.

Poisson's ratio was set to 0.4. Eventhough recommendations from Brinkgreve et al. (2014) indicate that for undrained cases, Poisson's ratio should be smaller than 0.35 (v ≤ 0.35) in PLAXIS. This is to make sure that the soil skeleton is more compressible than water and that the bulk stiffness of water (*Kw*) calculated should be lower or equal to the real bulk stiffness of the water (K^{0}_{W}) (Brinkgreve et al., 2014c).

Table 1.Soil characteristics and slope dimensions for the initial slope case used as reference for all programs

Parameters	Value	Unit
Unit weight (γ)	16	kg/m^2
Undrained shear strength (cu)	cu_0+2*H (H<8m)	kPa
Young modulus (E)	5	MPa
Drained shear strength (su)	2	kPa
Poisson's ration(v)	0,4	*dimensionless*
K_0	0,67	*dimensionless*
Total height	10	m
Base length	50	m
Slope height	5	m
Slope ratio V:H	1:2	*dimensionless*

It was necessary to establish a reference study of FOS, for which an analysis was done using the classical LE method for the case 1 (total stress based) and it was compared to both FEM softwares. Given the general familiarity there is with LEM, it is essential to establish how much dissimilarity from this can be expected from using FE, this way a reference from a known practice is set.

First the model was built using PLAXIS, later it was replicated in both SLOPE/W and COMSOL-Multiphysics, only for case 1 (total stress based). The second case (effective stress based) was only analysed using PLAXIS and COMSOL. The same geometry was used in both cases.

The safety analysis was done using SRM. The preliminary value used to compare each FE program was the FOS. Then, as part of a more detailed comparison of both programs, a series of stress points located along the failure surface generated (zone of maximum displacements) were studied.

These points were first selected from PLAXIS, since it is possible to access the nodes and stress points of each element in the mesh. In COMSOL nodes and stress points cannot be accessed due to the multi-physics nature of the program. The coordinates (X,Y) from each stress point were taken from PLAXIS and, by means of using *domain probe points*, the same were replicated in COMSOL. Graphs comparing stress paths were generated using a simple series of excel sheets.

5.1.1. LEM analysis

Using SLOPE/W as a computational tool, a LEM analysis of the case 1 (total stress based analysis) was performed for which some assumptions had to be done. The LE analysis is to be performed with Spencer's method, since this is recommended by Griffiths and Lane, (1999) who indicate that "*there seems to be some consensus that Spencer's method is one of the most reliable*" (Griffiths and Lane, 1999). Attention should be paid that a coarse-grained soil maximum slope angle should not exceed effective friction angle (Budhu, 2012).

The critical slip surface was produced by the automatic generation option. The minimum slip surface and factor of safety tolerance were left as default, 0.1 and 0.01 respectively. The number of slices was set to 60. As for the optimization settings, these were all left as default. For the FOS distribution no probabilistic distribution was used.

5.1.2. FEM analysis

A plane strain model is considered to be enough approximation of reality and this was set with both programs, PLAXIS 2D and COMSOL. In both FEM programs a 15-noded triangular element mesh is used, initially a coarse mesh will be used followed by a refinement, to estimate the effect of the mesh size in the calculations.

For both programs, boundary conditions were defined by free on the top boundary, roller on both lateral boundaries and fixed constraint at the bottom.

To examine the stress paths, *s':t* curves were plotted for the previously selected stress points. In PLAXIS, these graphs can be directly generated from the graph options for output display of information. In COMSOL, diagrams were plotted from the information in the *domain probe points,* obtained by interpolation between gauss or nodes points to each *domain probe point* in each element. However, some discrepancies appeared in the process and finally data was extracted and handled through excel sheets.

It is worth remarking that eventhough gravity is considered as 9.81 m/s^2 in both programs, the unit weight of water is 10 [kN/m^3] in PLAXIS while in COMSOL is 9.81[kN/m^3]; therefore, results are expected to deviate slightly when water table is taken into account in the analysis, for example pore pressure values (u) and consequently effective stresses (σ').

PLAXIS

Through the *Boreholes* feature, soil properties per layer, water table (when applicable) and slope geometry (height and inclination), were established for both cases. The elastic perfectly-plastic Mohr-Coulomb criterion was used. Depending on the case studied either *drained* or *undrained B* conditions were applied. K_0 was calculated based on the selected value of Poisson's ratio ν = 0.4.

COMSOL Multi-physics

Under the *Structural Mechanics* branch, the interface of *Solid Mechanics* is available and was used to analyse the slope. Using the *Soil Plasticity* sub-node (available under the *Linear Elastic Material* node), the soil characteristics were defined using the yield criterion based on the Mohr-Coulomb model. The initial stresses are studied based on gravity loading and initial strain were set to zero.

The model was discretised using quartic elements which are equivalent to 15-noded elements in PLAXIS; the mesh was established as controlled by the user, to be able to adjust the size of elements in accordance to PLAXIS, and free triangular elements were selected. It should be kept in mind that the discretisation has to be defined in each *physic* (or branch) added and these should match to each other in order to avoid locking the mesh.

The safety analysis based on SRM cannot be set directly in the program; instead the reduced values of shear strength indicated with *c*, cohesion intercept (c_c') and the effective angle of internal friction (ϕ_c'), are defined as functions of the FOS by:

$$c'_c = c'[kPa]/FOS$$

$$\phi'_c = atan(\tan(\phi'[deg]))/FOS$$

Where *c'* represents the initial value of the shear strength and it is expressed in terms of kPa; and *φ'* refers to the initial value of effective internal friction angle, which by default is accounted in radians [rad] but it can be set to degrees [deg]. FOS is defined as variable in the parameters section indicating a value of 1 and the unit as 1 (indicating dimensionless value). Later, through a parametric sweep, the FOS value is slowly increased from an initial value (usually 1) until a limit value is reached (2-3) depending on the case. The gradual increase is defined by a step-size that the program must take; therefore *c*' and *φ* are progressively reduced. The damping factor and tolerance factor, as well as the number of iterations must also be set by the user and usually adjusted to reach a proper result.

5.2. Case study 1: reference study (total stress based analysis)

The case 1 (total stress based) was planned to be analysed by both FEM programs and compared to a conventional LEM using SLOPE/W program, as explained before.

The slope was modelled under *undrained B* condition analysis in PLAXIS; which is defined as a combination of effective stiffness parameters and total strength parameters (undrained).

Additionally two alternatives for the development of the slope were simulated, only for this case. In one scenario, the initial stresses were generated by the *gravity loading* method, representing a man-made slope such as road embankments. On the other, the initial stresses were created by the K_0*-procedure*, as simulating a naturally eroded slope from an initial soil mass to the final geometry. This was done to verify that both procedures would cause similar results for the initial stress and strain condition.

Additionally:

- No structural elements were added.
- No water table was evaluated, since pore pressures are not taken into account in the total based analysis.
- Simulations were performed using a normal mesh that was later refined so that the mesh dependency could be assessed. To see the mesh and soil parameters for this case, see *APPENDIX D: Summary of parameters and mesh adjustments for case 1.*

5.3. Case study 2: effective stress based analysis

This following case was done simulating a drained condition using effective strength and effective stiffness parameters. A water table of 2 meters below ground surface was set as indicated previously in Figure 10, which divided the entire geometry into two domains, see Figure 11. This case was analysed using only FE programs.

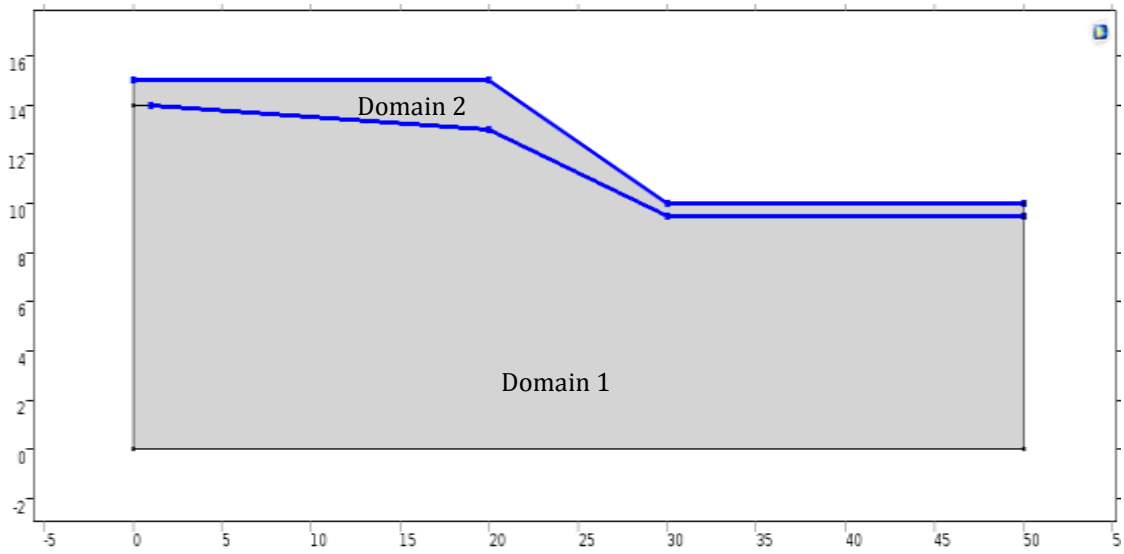

Figure 11. Slope model from COMSOL indicating 2 domains and the boundaries defined as pressure P=0kPa

In an equal manner to the previous case, a comparison of the effect of mesh size is evaluated. Initially a simulation of the slope was done with a coarse mesh in both programs and later compared to results after a mesh refinement was done.

The initial value for the drained shear strength was set to a 10% of the undrained shear strength (cu). However, later, it was found that the strength values chosen were too low resulting in several regions with plastic points in the initial stresses state, meaning that the Mohr-Coulomb failure criterion was being violated for the initial sate. Therefore, a higher value was ultimately used, eventhough this might no longer be representative of the local area typical soil characteristics.

Under PLAXIS, the slope was simulated using the *drained* option, indicating effective stress parameters and no effect of pore pressure. However, given some issues in the

setting of the model in COMSOL, this slope case was also compared to simulations done evaluating the material using *effective and total unit weight* and no water table.

Since it is not possible to directly indicate the water table in COMSOL, a *Darcy's Law* interface (physics) was added, where the pressure was defined in the boundaries of the geometry to simulate the groundwater conditions. To indicate the water surface, the corresponding boundaries were set to *Pressure* equal 0 kPa, see Figure 11. As for the lateral boundaries, it was added the node *Pressure Head* as a function of the height in meters of water corresponding to each lateral boundaries, 14[m] in the left boundary and 9.5[m] in the right boundary. These height values were defined in the *parameters* node, in the *Global* definitions, together with all other defined variables that were to be used in the rest of the model.

To proceed with the modelling under *drained* conditions (as it is specified in PLAXIS), in COMSOL it was necessary to include the effect of water pressure (*pw* in COMSOL). In a first *study*, Darcy's law was calculated and so the *pressure* in the initial phase. In a following *study*, the *solid mechanics* was analysed including the effect of the previous *study* (water pressure). To ensure the results would be in terms of effective stresses, the effect of water pressure is added to the *first invariant of stresses* (solid.I1.s) and to the *pressure* (solid.pm) equation which can be accessed in the *equation view* under *soil plasticity* node, or alternatively it can be added to the failure criteria given by the *yield function* (solid.Fyield) and the *plastic potential* (solid.Qplast) equation, see Figure 12. In the same manner, the value of pressure (*pw)* must be included in the *Initial stress and strains* node.

In a later analysis, a comparison of different settings for the same model was performed. It was decided to additionally compare the results from the *drained* settings to a model with *effective and total unit weight*, for domain 1 and 2 respectively, in the geometry shown in Figure 11, with no water table included. This was done in order to ensure the Poisson's ratio (v) was in terms of effective stresses, the total and effective density for the model were set to 16 kN/m^3 and 6kN/m^3 respectively. As well, the generated effective stresses and respective K_0 were assessed for a specific point in the model.

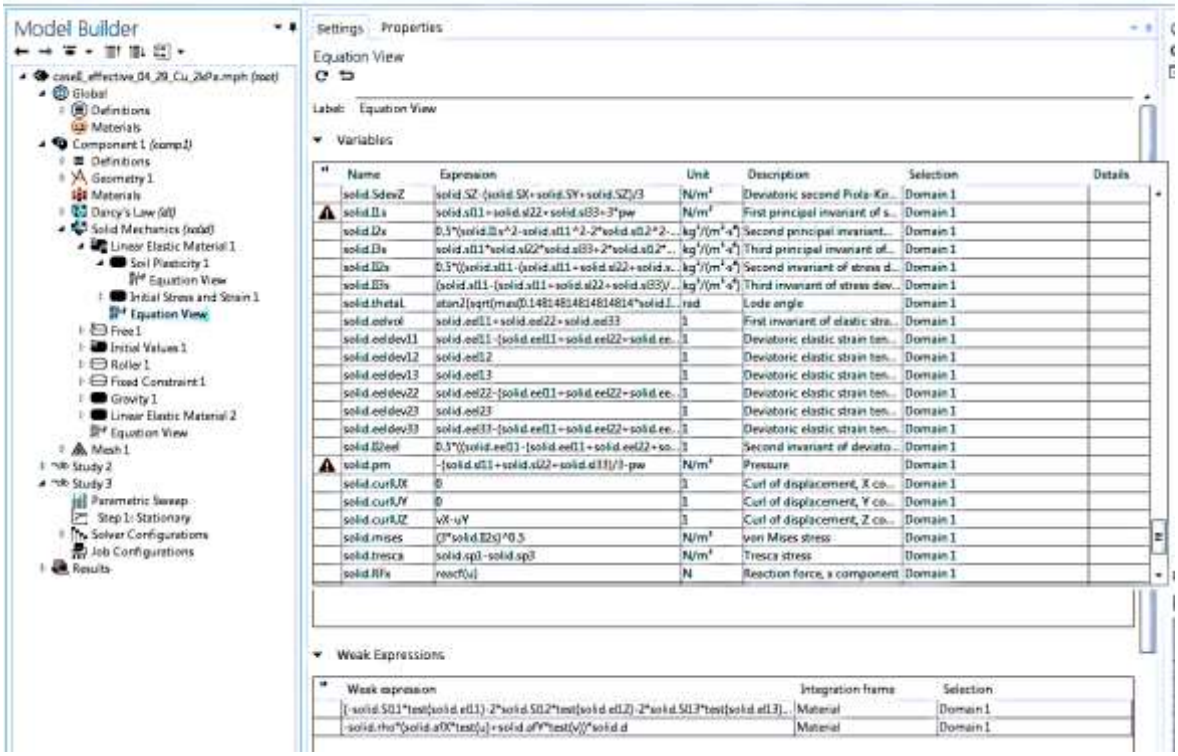

Figure 12. Example of user interface in COMSOL and adjustment of effective stress by adding the pressure variable to the first invariant of stresses and to the pressure equations.

Additional measures taken:

- Shear strength value finally used is 10kPa, 50% of cu, instead of the 2kPa, 10% of the undrained shear strength (cu).
- No structural elements were added.
- Different conditions were evaluated in both programs to ensure and evaluate *no excess pore pressure* condition and effective stress based analysis.
- The different element sizes and mesh refinement are summarized in *APPENDIX E: Summary of parameters and mesh adjustments for case 2* for each set of conditions tested.

6. RESULTS

The results of the studied cases, including outputs from the FE programs and the comparison of the stress paths generated, will be presented next.

Preceding the definition of the case 1, a set of fabricated parameters of strength and stiffness were particularly chosen and modelled in PLAXIS and SLOPE/W as a form of test of the programs.

A relatively acceptable FOS was reached with both tools. However, in a closer analysis of the resulting stress distribution for the initial state (not at failure); it was found that the slope itself was in an ultimate state, reaching the maximum shear strength almost in the entire model. The fabricated soil parameters were found to infringe the Mohr-Coulomb failure criterion; these were not validated before modelling the slope, since it was an exercise to familiarize with the tools.

In spite of this critical condition in the "natural" state of the slope, a FOS of 1.40 and 1.46 was obtained using SLOPE/W and PLAXIS respectively. It was not possible to foresee this initial state of failure by the use of LEM tool (in this case SLOPE/W) nor there was any warning displayed during the set-up and computation of the model in PLAXIS. This exposed the importance of knowledge of soil mechanics theories by the user, independently of which computational tool is used.

6.1. Case study 1: reference study (total stress based parameters analysis)

Only the relevant results of obtained FOS and stress paths will be presented next; nevertheless, relevant adjustments done and significant findings reached during the process will be mentioned.

6.1.1. Resulting FOS

The resulting FOS using both approaches, LEM and FEM, with the different programs are presented in Table 2. It can be observed variances between LEM and FEM are maximum 5%, which is considered to be within an acceptable range. In accordance to what it has been indicated by different authors such as Duncan, (1996) who pointed out that an accuracy of about $\pm$6% to be close enough for practical purposes given the uncertainties associated with soil properties. Therefore a maximum difference of about 5% can be thought to be fairly acceptable.

As well, the differences between both FEM programs are found to be approximately 2% for the drained conditions evaluated with a coarse mesh indicated under the column *mesh density* as *coarse*.

The FOS, using only FEM programs, was also analysed for a finer mesh option (higher mesh density) and results are presented in Table 2, where mesh is indicated as *fine*. As it can be observed, the difference between the reached FOS using both programs is less than 2%, which is to be expected since results should become closer in agreement the finer the mesh is.

Given the nature of the LEM, no mesh is created which is why it is indicated with *NA* (not applicable). As well, with LEM it is not possible to define stiffness parameters since these are not considered in the method, therefore the Poisson's ratio (v) is indicated in the table as *NA*, to indicate that no value was used in the calculations done with SLOPE/W.

Table 2. Resulting FOS for case 1 (total based analysis) with a fine mesh option, indicating difference between each program

Condition	cu kPa	ϕ	v	Mesh density	Program	FOS	Difference	
							FEM-FEM	FEM-LEM
total stress analysis	20+2*Z	0	0.4	coarse	PLAXIS	2.106	2.06%	2.93%
	20+2*Z	0	0.4	coarse	COMSOL	2.149		5.05%
	20+2*Z	0	NA	NA	SLOPE/W	2.046		
	20+2*Z	0	0.4	fine	PLAXIS	2.103	1.83%	
	20+2*Z	0	0.4	fine	COMSOL	2.142		

6.1.2. About the tools used

As indicated in section 3.1, the resulting FOS using LEM depends on many assumptions that must be made initially, such as defining the slip surface before calculations. For the analysis of case 1, which was the only case analysed with LEM, some of the evaluated critical surfaces during the process are shown in Figure 13, for each calculated slip surface a different FOS is reached. Due to space and relevance for the matter not all the slip surfaces and FOS generated will be shown. The final slip surface and FOS would be related to the most critical FOS value found (the lowest value).

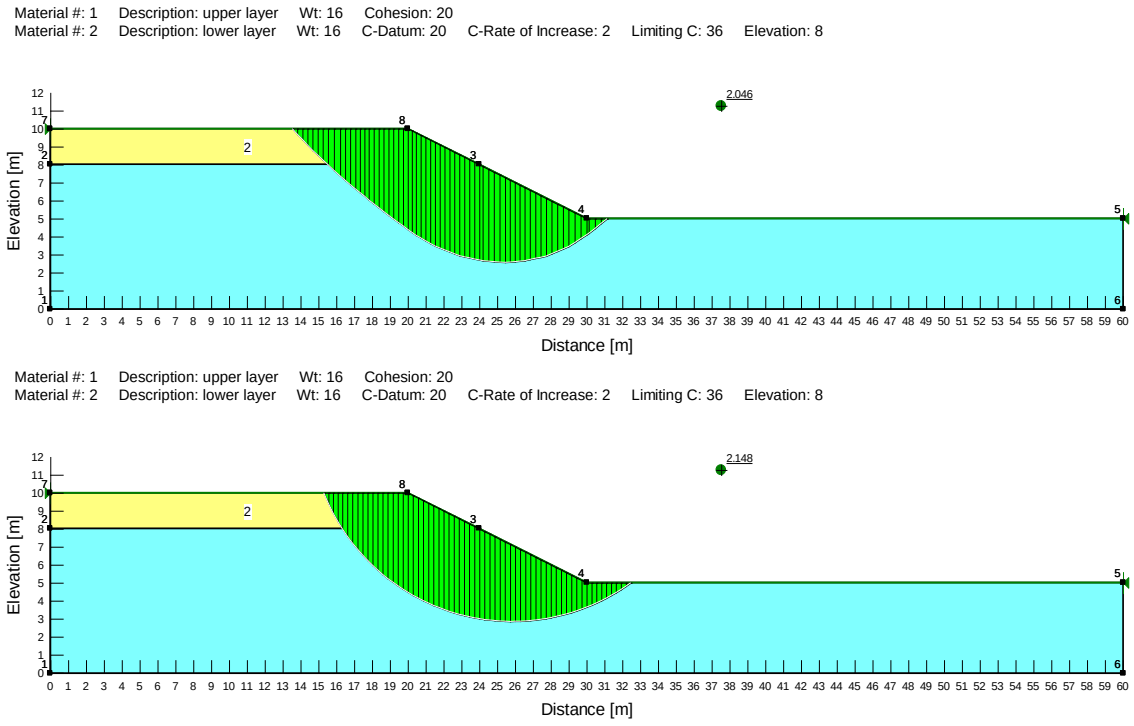

Figure 13. Resulting FOS from two slip surfaces generated as part of Spencer's method

6.1.3. Stress paths analysis

The case 1 was modelled using both programs COMSOL and PLAXIS. A comparison of the stresses generated by both programs in specific points was done. Since critical slip zones (major displacements) had small differences between both programs, these were superposed one with the other to ensure that the stress points selected for the analysis were inside the critical failure zones created both in PLAXIS and COMSOL. An example of the generated critical slip surface (major displacements) in PLAXIS and the points selected along this surface can be seen in *APPENDIX A: Slip surfaces in PLAXIS and the selected stress points within failure zone for case 1.* The colour red indicates the highest displacements which gradually turn into deep blue (no displacements). The points indicated are the ones for which *s:t* curves were generated.

In Figure 14, it is shown the different curves generated for each of the selected points with both programs. In general, curves are rather similar, except for point 1 (17.22, 9.58) which appears to have almost an opposed behaviour, indicated in the dotted square.

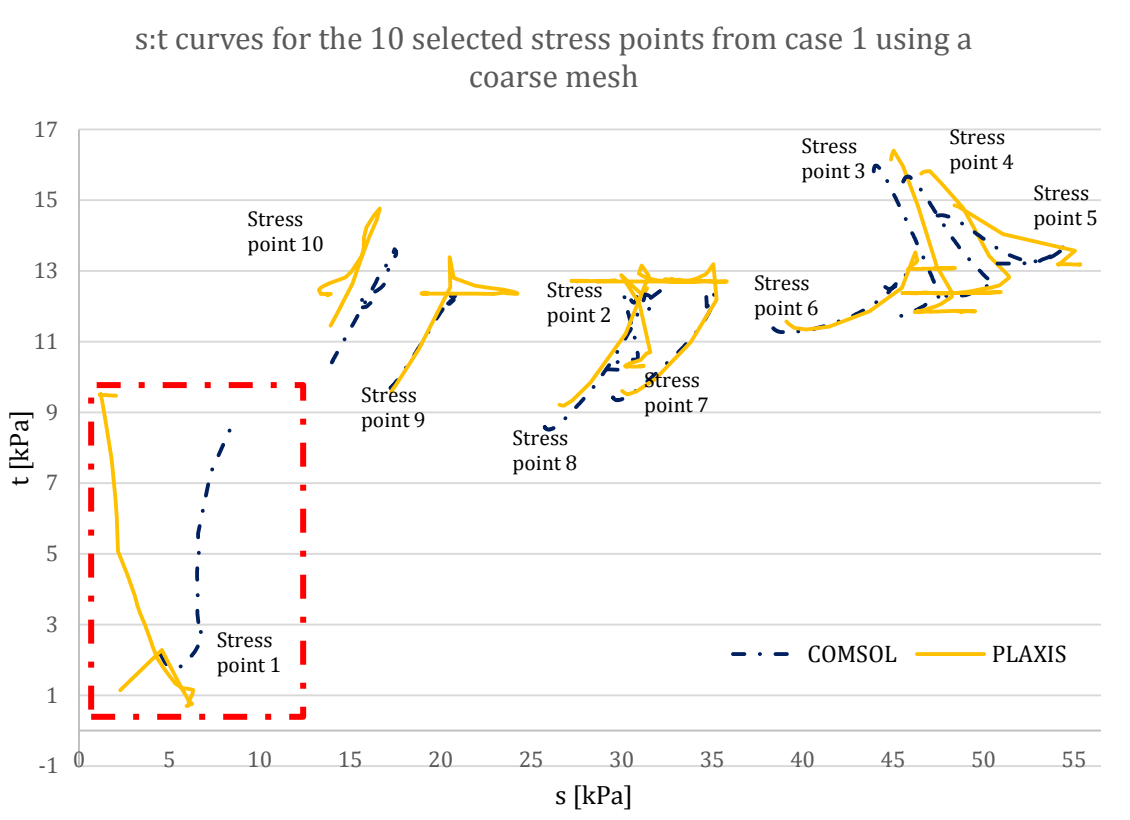

Figure 14. Stress paths (s':t curves) of 10 selected points along the slip surface of case 1 slope with coarse mesh

It was decided to further analyse point 1 (17.22, 9.58). A closer examination was performed by first choosing several stress points in close distance to this specific point; and later by generating the corresponding *s':t* curves initially only in PLAXIS. It was found that points in close distance showed somewhat dissimilar behaviours.

It was then decided to verify if the same erratic performance was observable using COMSOL. In order to create and compare curves in both programs, a similar procedure as for choosing the initial selected points was done; by first selecting the points in PLAXIS and taking the coordinates to COMSOL and creating *domain probe points*.

These points were then plotted to be compared and are shown in Figure 15. As it can be appreciated, in COMSOL points seem to behave similarly while curves generated in PLAXIS perform differently, in spite of using the same program, under the same soil conditions, mesh elements and size.

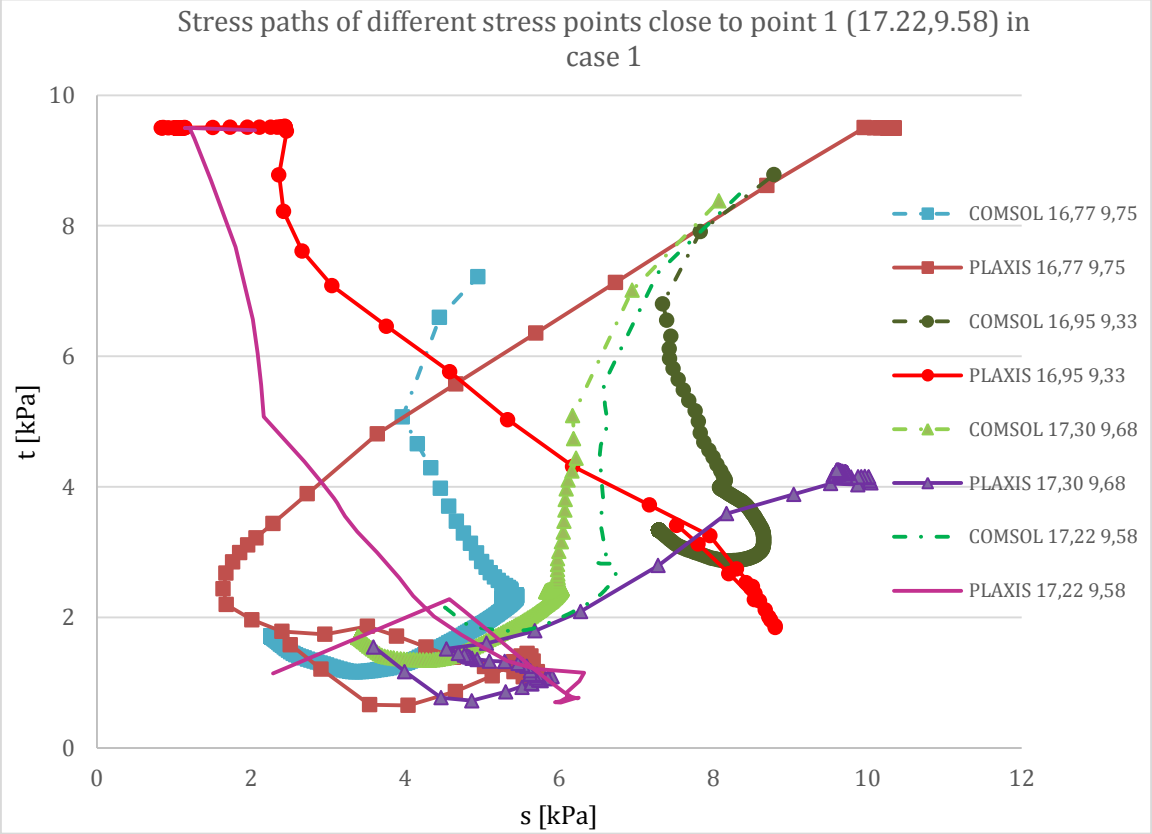

Figure 15. Sensitivity analysis of points around stress point (17.22, 9.58) using PLAXIS and COMSOL to observe closer the behavior.

However, later it was found that analysis done in COMSOL using gauss points differed considerably from using nodes stress points. Considering that *s-t'* curves were plotted directly from the programs and the differences in the conventions for minor and major principal stresses (σ'1 and σ'3) of the programs, it was decided to obtain directly the values of the major and minor principal stresses (σ'1 and σ'3) instead of *s-t'* curves. Like before, it was found that for most points, curves from both programs were in good agreement, except for point (17.22, 9.58).

Curves generated from data extracted from the nodes in COMSOL matched the behaviour and tendency as the ones produced from data from the stress points in PLAXIS. However, graphs created from data extracted the gauss points in COMSOL behaved slightly different, but only for point 1 (17.22, 9.58) as shown in Figure 16.

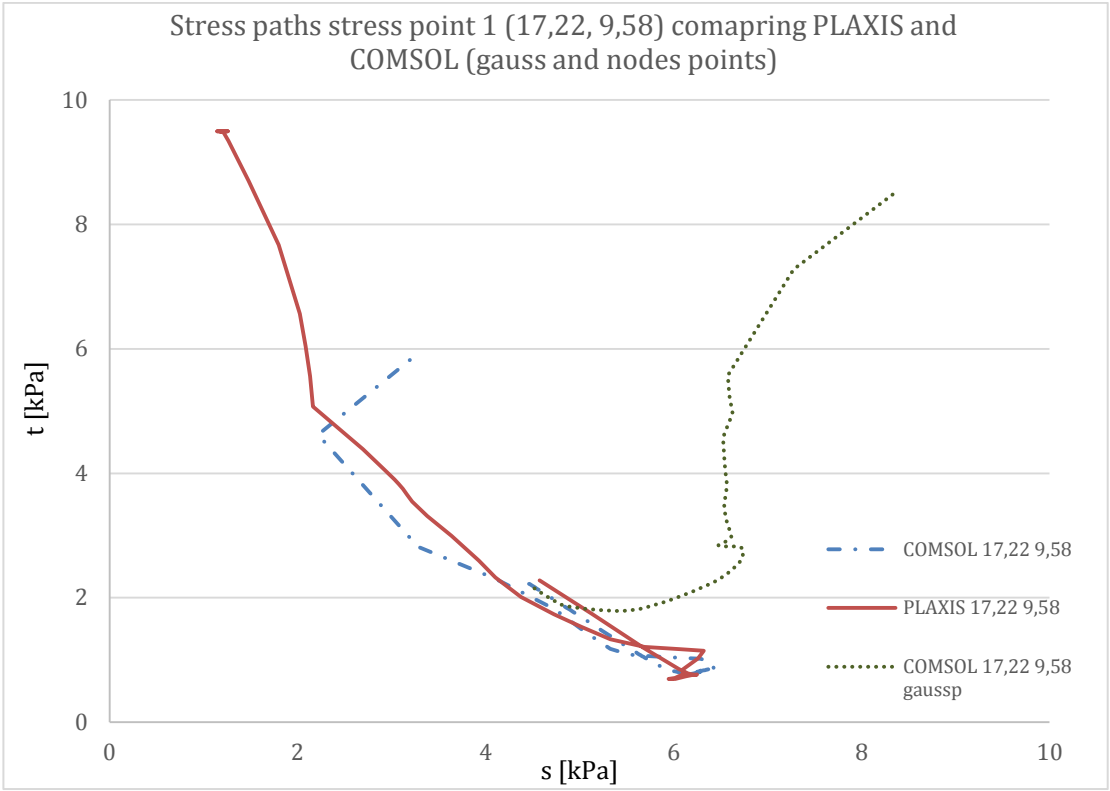

Figure 16. s':t curves generated for a closer evaluation of point (17.22 9.58) using data from PLAXIS and COMSOL.

Since in COMSOL it was used *domain probe points* instead of directly selecting stress points in the element, it is possible that the difference is due to the interpolation procedure between the nodes and the *probe points* and between the gauss points and the *probe points*. Therefore if a finer mesh (smaller elements) is used, interpolation from nodes and gauss points should be in closer agreement.

6.1.4. Stress paths analysis with finer mesh

A finer mesh was then evaluated to examine if previous dissimilarities between stress paths generated remained. A refinement was done in PLAXIS by setting the *relative element size;* while in COMSOL, the maximum and minimum element size was adjusted until an approximate same number of elements and size of elements was achieved. The analysis was repeated to select points along the critical surface (major displacements, the points selected and mesh density can be seen in *APPENDIX B: Slip surface in PLAXIS and the selected stress points along the failure zone for case 1 with a finer mesh*. A new set of *s':t* curves were generated for different stress points in the new critical zones created in both FE programs, see Figure 17.

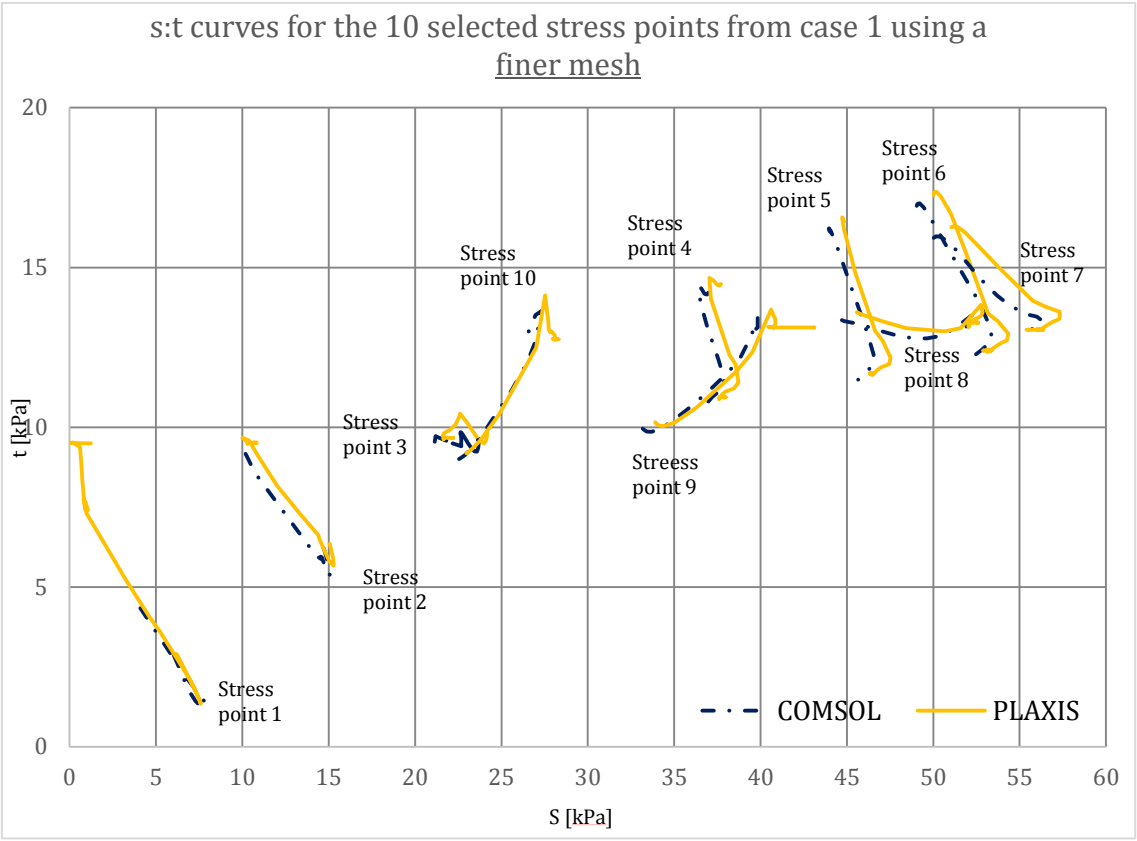

Figure 17. Stress paths (s':t curves) of 10 selected points along the slip surface for case 1 with a finer mesh

A similar sensitivity analysis was performed to a point located as close as possible to previous point 1 (17.22, 9.58), from the coarser mesh examination. Stress point 1 (17.27 9.44) was selected and several others surrounding this point. The curves generated are shown in Figure 18, and, as expected for a finer mesh, both programs show similar behaviour for all points.

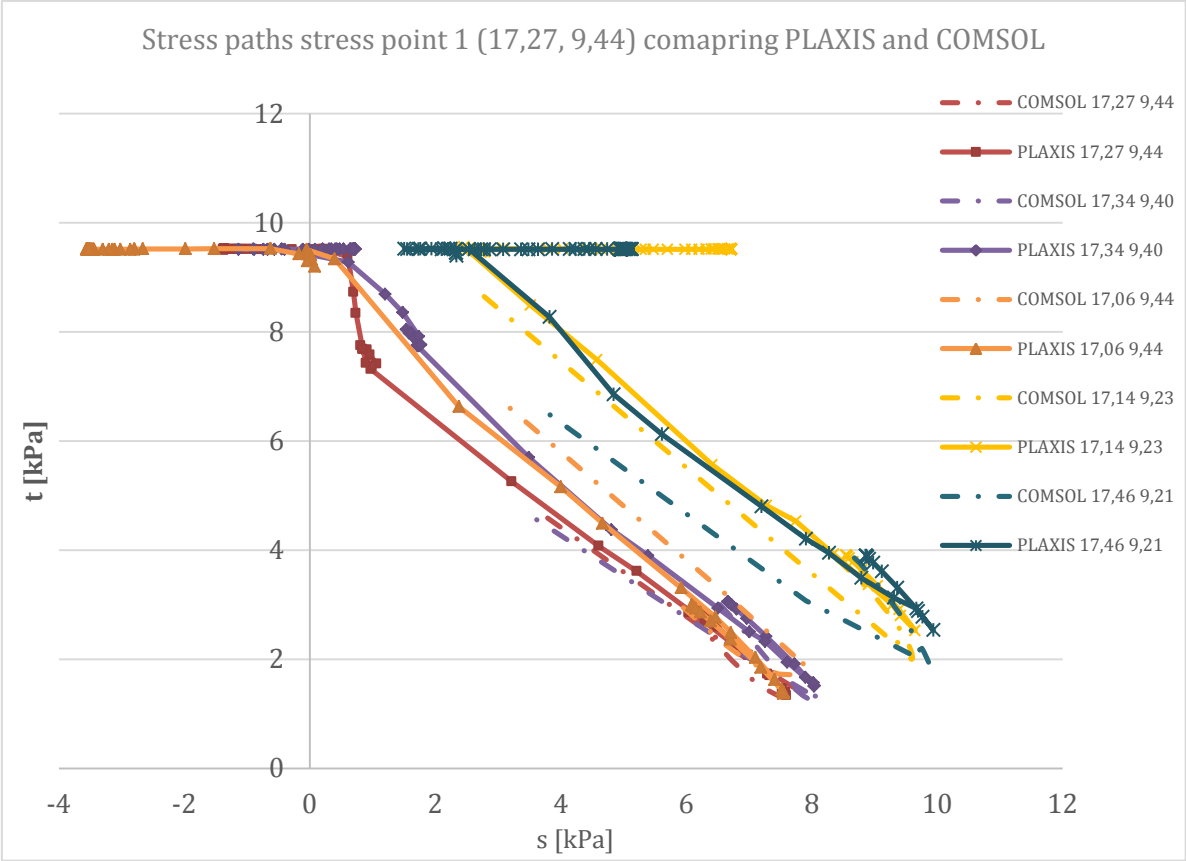

Figure 18. Sensitivity analysis of points around stress point (17.27, 9.44) using PLAXIS and COMSOL to compare the behavior of points.

It is observable that with the refinement of the size of elements in the mesh, values of principal stresses at the chosen points become closer in behaviour and values. This is expected since the smaller the element the closer the points are within each element.

6.1.5. Discussion

On the resulting FOS showed in Table 2 it is observable a small difference in the outcomes from both FE programs. It can be guessed that the fact that mesh elements are not exactly in the same position, consequently neither are the nodes nor the stress points, influences to a certain extent the difference in results; since it is not possible to control the meshing process in none of the softwares.

Another factor of influence could be the type of solver used. In PLAXIS is not possible to neither access nor modify the settings of the algorithms or equations; therefore calculation procedures are not done exactly the same in both softwares. In spite of these discrepancies, the differences between the programs are quite minor for the case 1 (total stress based analysis) and it can be considered that results are in very good agreement.

The reduction in the difference between the resulting FOS, from PLAXIS and COMSOL, is to some extent related to the mesh density. As well, the erratic behaviour for a specific point located in the slip surface is no longer observable when the mesh size is

reduced, which it is to be expected since the interpolation from the gauss points (stress points) to the selected points becomes more accurate since distances are smaller (smaller elements).

About the points showing an inconsistent behaviour in PLAXIS, it is presumed that these points might be located in exactly the slip surface. It is possible that the selected stress points were placed in different elements which deformed in different directions (sliding material), meaning that different points within the same element may be displaced in diverse directions. And, as indicated above this discrepancy disappeared once the mesh density changed (smaller elements) and stress points were closer together.

An additional examination was performed considering the selection of the stress points from the total deviatoric strain band generated in the slope instead of the failure surface.

A comparison of the stress paths from both programs was done, see Figure 19. As it can be observed, the behaviour of the curves is in very good agreement for all selected points, in spite of being a coarse mesh. As well, no inconsistent behaviour was found for points close to the top surface of the slope as it was found before.

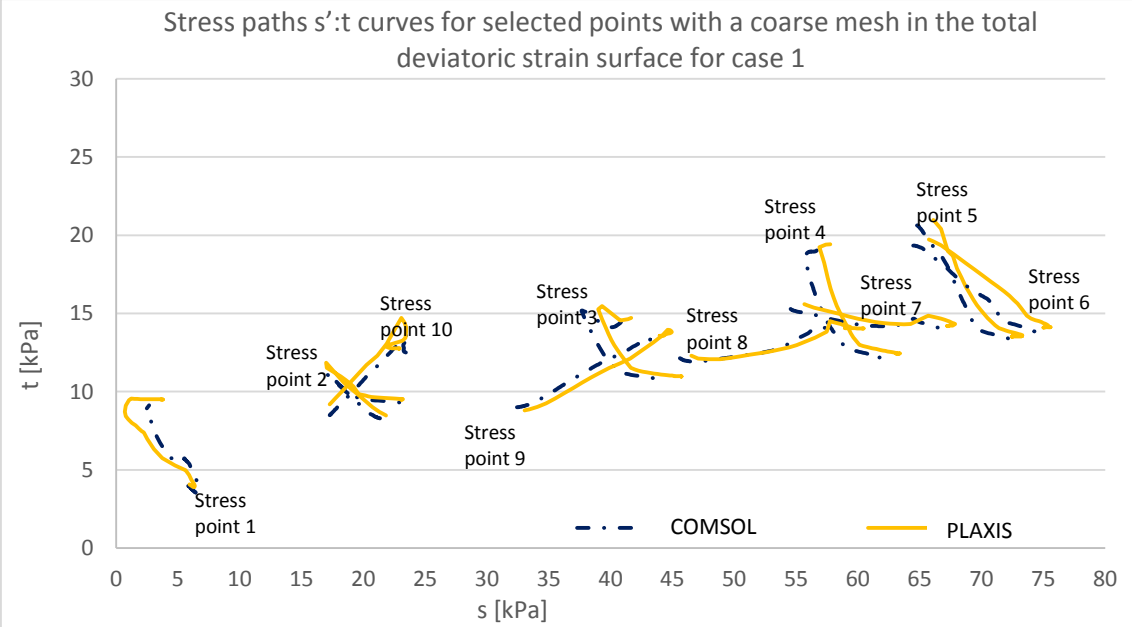

Figure 19. Stress paths (s':t curves) of 10 selected points along the strain surface of case 1 slope with coarse mesh

6.2. Case study 2: effective stress parameters

As part of the case 2, the same geometry as in case 1 was used; and as indicated before effective stress and effective stiffness based parameters were used.

It was specified previously that in PLAXIS the slope would be analysed using the *drained* condition available in the software. During the modelling with both programs, PLAXIS and COMSOL, evident differences were found both in the resulting FOS and the failure surface; therefore, it was decided to test different settings to simulate effective

stress conditions. This was done by evaluating the model using different settings and combinations of these. A *drained* analysis and an analysis using *effective and total unit weight* without considering the water able were performed considering different values of shear strength and different mesh sizes. Resulting FOS from all approaches will be presented next.

Since several obstacles were encountered while setting this case, only the relevant results of both FOS and stress paths will be presented; nevertheless, relevant adjustments and significant findings completed during the process will be mentioned.

6.2.1. Resulting FOS

Results from modelling under *drained* and *effective and total unit weight* condition, including both evaluated values of drained shear strength and different mesh densities are presented in Table 3. FOS was evaluated using only FEM programs (no LEM was used).

As it can be observed the maximum difference encountered between both softwares is approximately 5%; this was for the *drained* condition analysis with 2kPa of shear strength and a coarse mesh.

The closest FOS agreement was found when evaluating *total and effective unit weight* with 10kPa shear strength and a fine mesh, showing a difference of 2.03 % between both programs.

It can be observed that FOS obtained for the *drained* condition analysis is always lower values than when evaluating directly *total and effective unit weight*.

Table 3. Summary of tested settings for case 2 (effective stress based analysis) and resulting FOS

Condition	Cu kPa	ϕ	v	Mesh density	Program	FOS	Difference
effective densities	2	30	0.4	coarse	PLAXIS	1.580	2.53%
	2	30	0.4	coarse	COMSOL	1.540	
	2	30	0.4	fine	PLAXIS	1.545	2.27%
	2	30	0.4	fine	COMSOL	1.510	
	10	30	0.4	coarse	PLAXIS	2.730	2.56%
	10	30	0.4	coarse	COMSOL	2.660	
	10	30	0.4	fine	PLAXIS	2.705	2.03%
	10	30	0.4	fine	COMSOL	2.650	
effective stress	2	30	0.4	coarse	PLAXIS	1.361	5.66%
	2	30	0.4	coarse	COMSOL	1.284	
	2	30	0.4	fine	PLAXIS	1.316	NA
	2	30	0.4	fine	COMSOL	NA	
	10	30	0.4	coarse	PLAXIS	2.079	3.27%
	10	30	0.4	coarse	COMSOL	2.011	
	10	30	0.4	fine	PLAXIS	2.071	3.24%
	10	30	0.4	fine	COMSOL	2.004	

From Table 3, it can be observed that in most cases when the mesh was refined the results showed a smaller difference. However, when using the shear strength of 2kPa, no result was reached using COMSOL which is denoted by *NA* (not applicable) since no results could be reached. This is expected since the shear strength value generated plastic points in certain regions of the slope when verified in PLAXIS.

However, it is important to remark that FOS>1 were reached with all settings evaluated, even for the conditions where plastic points appeared in the initial state.

6.2.2. Stress paths

The selected points along the slip surface can be observed in *APPENDIX C: Slip surface in PLAXIS and the selected stress points along the failure zone for case 2 (effective stresses).* Results from stress paths generated for 10 selected stress points in the failure surface (major displacements) for case 2, analysed under *drained* conditions in PLAXIS are presented in Figure 20. As it can be seen the behaviour of curves from both programs is somewhat similar, however curves are distant from being in good or fair agreement as for case 1.

In a closer look at each pair of curves from PLAXIS and COMSOL for each point, it is possible to observe that both curves present similar shape and behaviours, although they are distant from being the same. This is probable related to the coarseness of the mesh and the interpolation process to obtain data for the *domain probe points* used in COMSOL.

The *s':t* curves of each point were plotted to show these similarities in shape, values and behaviour, and the case be seen in Figure 25 - Figure 34, in *APPENDIX F: Different stress paths s':t curves for selected points in case 2: effective stress based analysis.* It can be seen that curves from both programs usually begin in a similar point, indicated by a square for COMSOL and a circle for PLAXIS, as well as these show an alike shape but with a significant distance between each curve and each initial point.

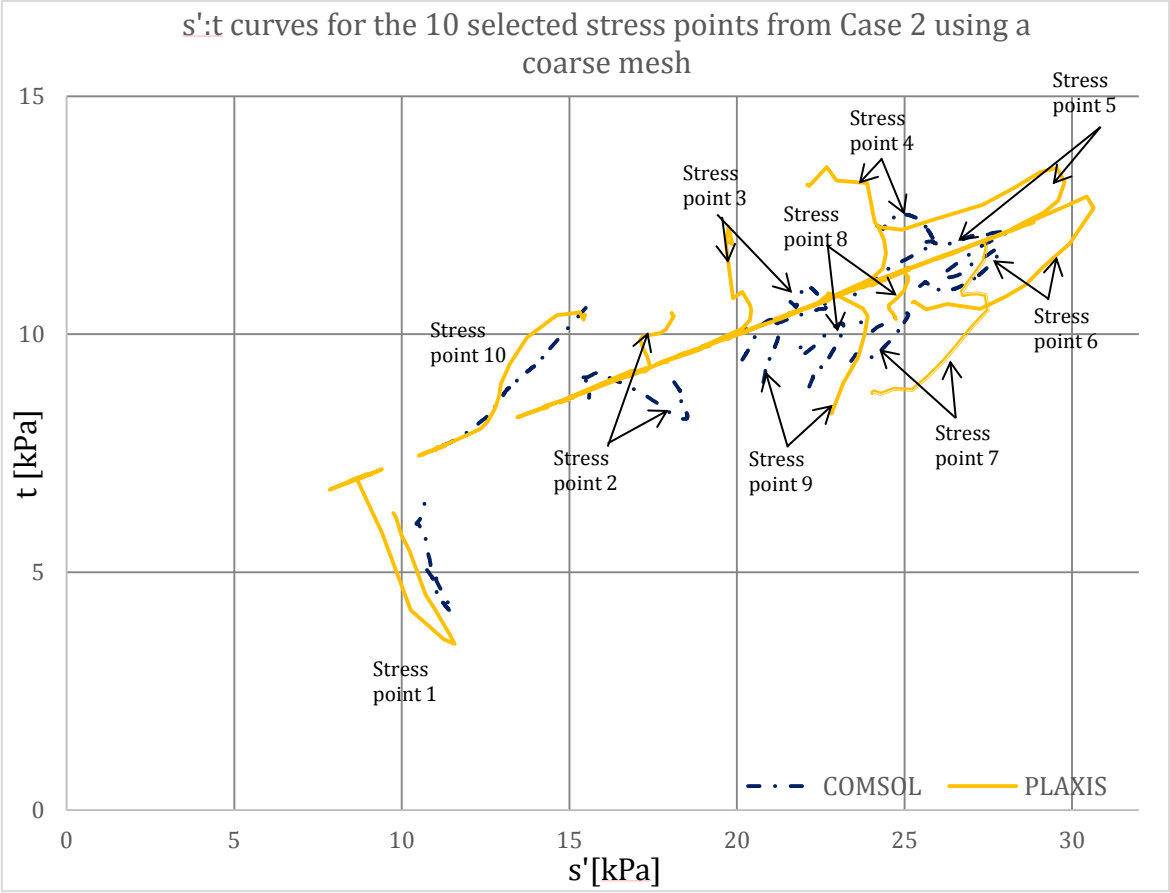

Figure 20. Stress paths (s':t curves) of 10 selected points along the slip surface of case 2 slope with coarse mesh

It can be observed as well that only selected points that are above the water table, point #1 and point #10 in *APPENDIX C: Slip surface in PLAXIS and the selected stress points along the failure zone for case 2 (effective stresses).)*, have a behaviour that can be considered in good agreement. As well, the curves generated for both points using both programs are closer to each other than the rest of points.

6.2.3. K_0-procedure and gravity loading for initial stress generation

As a form of pre-study for case 1, two alternatives for generating the initial stresses in PLAXIS were evaluated, *gravity loading* and *K_0-procedure*; although the latter is specifically not recommended to be used for slopes in PLAXIS, according to the reference Manual. Eventhough, both procedures are somewhat different minor differences were obtained in the different stress distributions, the mobilised shear stress (τmob) and in the total displacements (μ) generated; similarly the resulting factor of safety (FOS) was the same for both situations.

For the case 2, a similar assessment was performed, analysing the vertical and horizontal effective stresses (σ'_v and σ'_h respectively) for a specific point in the slope using both programs, and later calculating the K_0. The initial analysis was done to ensure that parameters defined in both programs, specifically the Poisson's ratio (ν),

were in fact in terms of effective stresses. The latter study was performed to assess that the obtained K_0 matched the initial defined value.

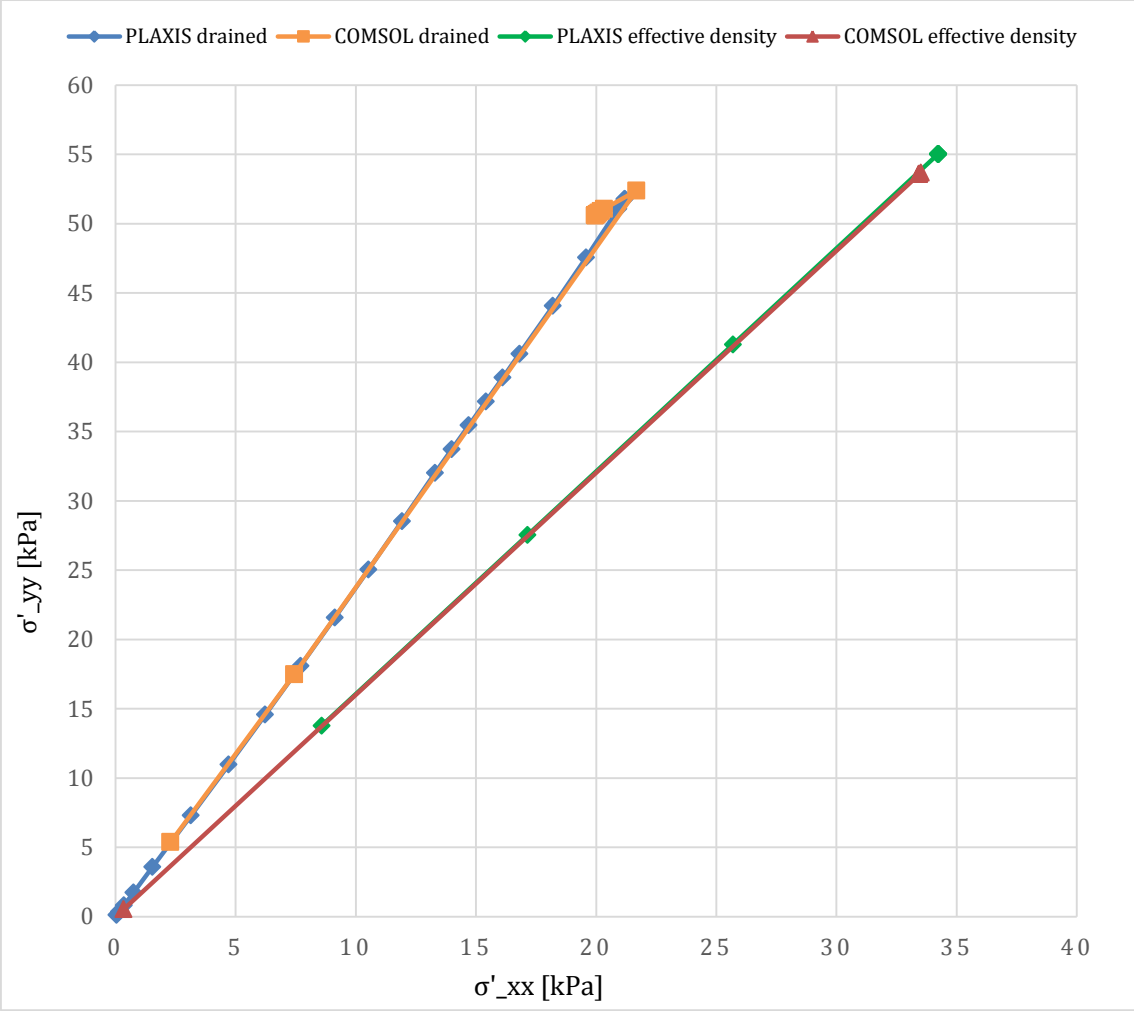

Figure 21. Vertical and horizontal effective stresses for a specific point (0.15, 7.7) for the initial state of the slope generated for *drained* conditions and *total and effective unit weight* using both FE programs.

From Figure 21, it can be observed that the data extracted from both programs are in very good agreement for each condition evaluated, *drained* and *effective and total unit weight*. From the ratio between the horizontal effective stresses to vertical effective stresses K_0 is obtained, and as it can be regarded there is a difference depending on the settings used; as well the values of the effective stresses are different although the trend obtained is similar.

6.2.4. Discussion

Initially a value of a 10% of the undrained shear strength was used to analyse case 2. However, due to the generation of several regions of plastic points in the slope for the initial state, it was then assumed a higher value of 10kPa (50% of cu), that as said before it is not related to the soil in the west region of Sweden.

It is important to remark that FOS>1 was achieved when analysing the case for 2.0kPa in PLAXIS, which denotes a stable slope case; eventhough the natural state of the slope was actually at failure. This is very important to highlight since the safety analysis indicated a "safe "slope, which again brings the matter of the importance of the knowledge and experience on the user for analysing and post-processing data.

For the same condition of 10% of undrained shear strength, in COMSOL, when using a coarse mesh results were obtained in close agreement to PLAXIS; however, once the mesh was refined it was not possible to start the simulation. This should be expected, since there was an initial state of failure, and it was an indication that the parameters should be re-evaluated and checked.

Once a closer evaluation of the K_0 was done, it was established that horizontal and vertical effective stresses for the point studied were in very good agreement for both programs, as well as the calculated K_0. However, the value for the selected point did not agree with the initial settings, which should have been K_0=0.667 for ν=0.4. This was later found to be related to the *gravity loading* procedure for generating the initial stress state which affects differently the estimated horizontal effective stress (σ'_h), especially in the presence of groundwater.

Initially several difficulties were encountered while setting up the model for case 2 and getting close results from both programs. Two different settings were used to analyse the model in terms of effective stresses. It was decided to evaluate the model using a *total and effective unit weight* and a *drained* simulation. Though similar results of FOS and failure surface were achieved for each situation with both programs, the difference between both settings is not fully understood. This is probably related to the gravity loading, and to the SRM method and the Mohr-Coulomb criterion instead of related to the programs, since both programs seem to result in similar out comes.

Unexpectedly, the difference is appreciable once the water table is included in order to generate the effective stress in the material. Therefore, it can be deduced that the SRM under the *drained* condition is affected by pore water pressure, eventhough final display of effective stresses and pore pressure indicate otherwise when compared to a setting of *total and effective unit weight*.

6.3. Lessons learned

As indicated initially in the results section, a form of pre-study was carried out to familiarise with the softwares. It was found that a result of FOS>1 was obtained for both methods (LEM and FEM) and softwares (SLOPE/W and PLAXIS) tested, eventhough the initial state of the slope created was at failure. This led to the conclusion that both programs can erroneously reach a value of "safety" without any display or warning that initial state shows collapse. Therefore, it is highly relevant the user's knowledge of the program and the mechanisms of calculations.

On the one hand, PLAXIS offers a friendly user-interface where the step-by-step is already given by the software; on the downside it is not possible to access the solvers used and settings, element types and discretisation, soil models or equations used, nor

alter any of these. On the other hand, COMSOL offers the possibility to access all equations, algorithms, as well as adapt to user's need any physics, studies, solvers and equation of the models used; on the downside, it is required that user knows about numerical analysis as well as *Geomechanics* to properly built up a model, it is not possible to access directly nodes and stress points in the element making difficult the comparison of information for single stress points, since the interpolation process to *the probe points* alters the results.

COMSOL is a highly sensitive tool to changes done in either the step size, mesh element type or size. As well as any change in the input parameters, type of solver, or in the tolerance and damping factors, will generate an alteration in the outcome and in the processing; posing difficulties to even start the calculations and the possibility to make more mistakes as the model is set up.

In PLAXIS, results are sensitive to any changes in the default settings of the numerical solver section, resulting in long computation times and even in errors. It was found that increasing the number of steps, reducing size and tolerance would result in irregular trends of the FOS (Msf in PLAXIS), but same results were always reached. It was noticed that using the default settings will always result in faster calculation times.

In COMSOL, it might even be difficult to start a simulation, if parameters and solvers are not well defined, meaning that no criterion law is being violated, or even if an initial state is too close to be at failure. While in PLAXIS, it is always possible to run the set-up model and reach a result, even for cases where parameters may infringe a certain criterion, which was the situation for the study *case 2* with 2kPa shear strength, see section 6.2. These differences in the programs make it difficult to recommend one program or the other. However, it is highly relevant and crucial that the user is aware of the different advantages and limitations of each tool, when both setting up a model and post-processing the outputs.

Understanding of soil models, simplifications, assumptions, areas of application and shortcomings, is found to be vital to ensure proper use of the computational tools in general. Without knowledge on soil behaviour, modelling and even on how laboratory testing is performed, it becomes difficult to interpret out-puts and even more challenging to process and evaluate the data. As well errors of different kinds, due to numerical methods nature or to soil models, cannot be straightforwardly detected nor corrected; and therefore, there is a risk of misleading results. None of the FEM programs used in this work should be used as a design tool in absence of knowledge on Geomechanics.

To be able to handle both computational tools correctly and to understand the nature of certain changes in the results obtained, it is necessary, and almost compulsory, certain familiarity with numerical analyses methods, especially FEM. It is thought that knowledge in this area should be part of any engineering track. To be familiar with the theories behind the approximation methods available, whether is finite element (FE), finite difference (FD), discrete element (DE) and discontinuous layout optimisation (DLO), should be part of any engineering background, especially with the growing use of technology and computational simulations.

7. CONCLUSIONS AND RECOMMENDATIONS

Conclusions and final remarks from the work developed in the report are presented in the following chapter, followed by a list of suggestions to expand the investigation done.

7.1. Important remarks

Resulting FOS compared from LEM and FEM, for case 1, showed a maximum difference of 5%, see Table 2, which according to scientific sources is within the range of previous evaluations and comparisons.

FOS obtained from PLAXIS were found to be more conservative than from COMSOL for the case 1, with total stress based parameter, see Table 2. This means that FOS values were always lower using PLAXIS than COMSOL. The opposite was observed for case 2, final FOS results were more conservative using COMSOL than PLAXIS, see Table 3.

In general, resulting FOS and stress paths were found to be in close agreement using both FE programs. Differences were maximum approximately 6% and in average around 2%; as well stress path showed similar behaviour with a greater agreement the higher the mesh density (finer mesh).

For the case 1 (total stress based parameters), it was found that results from both programs are in very close agreement, both the FOS obtained and the stress paths analysed. The small differences can be due to the meshing process and the algorithms used in both programs. From this case analysed, total stress based or undrained, it can be concluded that both programs are suitable for safety analysis.

For case 2, effective based parameters; it was found that the settings in COMSOL are highly sensitive to small changes, especially with the solvers used and the step-by-step of the model which is decided by the user. The latter refers to adding a node or study before or after another, separating a study for each physic added or performed all computation in a single step, defining the materials in a separate node or within each physics used, the different options to define a geometry also influences the way calculations are performed. However, COMSOL is still a powerful tool for soil mechanics analysis, as long as the user is aware of all the settings that need to be regarded and the influence in the outcome.

For the analysis of the case 2, effective stress analysis, a peculiarity was found when two approaches for defining effectives stress model were used. A *drained* analysis was compared to a setting with *effective and total unit weight* analysis, which resulted in the same effective stresses for the safety analysis but different FOS and failure mechanism (critical slip surface). Influence of the presence of water when using gravity loading was found highly relevant in these differences.

A far too coarse mesh will fail to provide an accurate value, but it was found that the opposite, a far too fine mesh, would cause long calculation times and even some computational problems due to the amount of data that needs to be handled at a time. Therefore, awareness of the effect of the meshing in the outcomes is key when

modelling, as well as choosing the right mesh density and discretisation is crucial for accurate results in less time.

The only method used for safety analysis was SRM, and as indicated in the theory and in further recommendations, different alternatives should be evaluated. It was observed, however, that there is an influence of the water table during a *drained* analysis (effective stress based analysis). This became evident when simulations comparing an *effective stress* analysis to a *total and effective density* analysis the values of the resulting FOS differed substantially. Likewise, for both types of effective stress analysis the K_0 value was calculated and found to be different in the initial phase, which is thought to be related to the *gravity loading* method.

Similarly, non-convergence of the FE programs was used as a failure indication; although this is not an sign of a real failure, it is the most commonly used approach to define when a slope could reach a collapse state. Additional definitions are suggested to be evaluated in the recommendations section related to the literature survey perfoemed.

7.2. Recommendations

In order to carry out more realistic evaluations on the effect of different techniques in the assessment of the FOS, as well to achieve more reliable suggestions on which is the most appropriate method to apply for a specific situation, the following considerations are suggested to expand the presented work:

- Compare non-convergence failure approach to alternative failure mechanisms, using the already tested cases, including stress paths comparison. As exposed earlier in the text, several authors have suggested diverse options to define when failure has been reached, such as 1) extending the plastic zone from toe to top of a slope, or 2) the moment when a fast change in horizontal displacement of a specified node (or nodes) occurs.

- It is important to remark that through SRM a hypothetic state of collapse is evaluated; therefore it is strongly suggested as a possible next study to contemplate alternatives in which a slope is actually brought to collapse by adding different types of loading. Therefore, it is suggested to evaluate c/phi reduction method (or SRM) with alternative procedures for stability analysis, by for example a progressive increase of static loadings, dynamic loadings, seepage conditions and/or combinations of previous; as well as assessing results against the already evaluated cases. Real cases of slope failures occurred in the past, from which information of soils and triggering conditions are known, could be studied and examined comparing the real failure mechanism to what SRM will produce.

- As well, consider alternative geometries (steeper slopes) in combination with different soil properties layers (different stiffness and/or shear strength). Including, the case where a soft band (weak layer) is considered; since this case is reported by (Cheng et al., 2007) to portrait the most difficulties when applying SRM.

– Include dilation angle and expand to different soil types, including more frictional material.

– Evaluate different soil models other than Mohr-Coulomb, including anisotropic models; as well as, it can be extended to cases such as deep excavations.

8. REFERENCES

ASHCROFT, I. & MUBASHAR, A. 2011. Numerical Approach: Finite Element Analysis. *In:* DA SILVA, L. M., ÖCHSNER, A. & ADAMS, R. (eds.) *Handbook of Adhesion Technology.* Springer Berlin Heidelberg.

BRINKGREVE, R. B. J. & BAKKER, H. L. 1991. Non-linear finite element analysis of safety factors. *Computer Methods and Advances in Geomechanis*.

BRINKGREVE, R. B. J., ENGIN, E., SWOLFS, W. M., WATERMAN, D., CHESARU, A., BONNIER, P. G. & GALAVI, V. 2014a. *PLAXIS 2D Reference Manual- Anniversary Edition,* Netherlands.

BRINKGREVE, R. B. J., ENGIN, E., SWOLFS, W. M., WATERMAN, D., CHESARU, A., BONNIER, P. G. & GALAVI, V. 2014b. *PLAXIS 2014 General Information,* Netherlands.

BRINKGREVE, R. B. J., ENGIN, E., SWOLFS, W. M., WATERMAN, D., CHESARU, A., BONNIER, P. G. & GALAVI, V. 2014c. *PLAXIS 2014 Material Models Manual,* Netherlands.

BUDHU, M. 2012. SOIL MECHANICS AND FOUNDATIONS. *In:* JOHN WILEY & SONS, I. (ed.) *SOIL MECHANICS AND FOUNDATIONS.* 3RD ed. Arizona: JOHN WILEY & SONS, INC.

COMSOL MULTI-PHYSICS. 2015. *Geomechanics Module- Overview* [Online]. Stockholm. Available: http://www.comsol.com/geomechanics-module [Accessed 2015-02-24 2015].

CHEN, L. H., YU, S. & ZHANG, H. T. 2011. Discussion of Criteria of shear strength reduction FEM. *Advanced Materials Research,* 243-249**,** 1279-1282.

CHENG, Y. M., LANSIVAARA, T. & WEI, W. B. 2007. Two-dimensional slope stability analysis by limit equilibrium and strength reduction methods. *Computers and Geotechnics,* 34**,** 137-150.

CHENG, Y. M. & LAU, C. K. 2014. Chapter 2: Basic slope stability analysis methods. *In:* GROUP, T. F. (ed.) *Slope Stability Analysis and Stabilization New methods and insight.* Boca Raton: CRC Press.

DUNCAN, J. M. 1996. State of the Art: Limit Equilibrium and Finite-Element Analysis of Slopes. *Journal of Geotechnical Engineering,* 122**,** 577-596.

DUNCAN, J. M. & WRIGHT, S. G. 2014. Chapter 3: Soil Mechanics Principles. *In:* JOHN WILEY & SONS, I. (ed.) *Soil strength and slope stability.*

FREI, W. 2013. Solutions to Linear Systems of Equations: Direct and Iterative Solvers. *COMSOL Blog* [Online]. Available from: https://www.comsol.de/blogs/solutions-linear-systems-equations-direct-iterative-solvers/ 2015].

GLAMEN, M. G. S. & NORDAL, S. 2005. View on stability and calculation methods. *Landslides and Avalanches: ICFL 2005 Norway- Senneset, Flaate & Larsen (eds).* London: Taylor and Francis Group.

GLAMEN, M. G. S., NORDAL, S. & EMDAL, A. 2004. Slope stability evaluations using Finite Element method. *In:* NGM 2004, T. A. P. (ed.) *NGM 2004 XIV Nordic Geotechnical Meeting May 19th - 21st 2004.* London: Sevnska Geotekniska Föreningen (SGF).

GRIFFITHS, D. V. & LANE, P. A. 1999. Slope stability analysis by finite elements. *Geotechnique,* 49**,** 387-403.

JAMISON, W. R. 1992. Stress spaces and stress paths. *Journal of Structural Geology,* 14**,** 1111-1120.

JOHN B. WATCHMAN, CANNON, W. R. & MATHEWSSON, J. 2009. *Mechanical properties of ceramics*, John Wiley and Sons.

KARSTUNEN, M. 2014a. Numerical modelling2. Geotechnical modelling II-BOM041 Infrastructure Geo-engineering. Lectures. Chalmers University of Technology.

KARSTUNEN, M. 2014b. Numerical modelling-BOM041 Infrastructure Geo-engineering. Lectures. Chalmers University of Technology.

KHOSRAVI, M. & KHABBAZIAN, M. 2012. Presentation of critical failure surface of slopes based on the finite element technique. *Journal of Geotechnical and Geoenvironmental Engineering*.

KNAPPET, J. A. C., R.F 2012. Craig's Soil Mechanics. *In:* PRESS, S. (ed.) *Craig's Soil Mechanics.* 8th ed. New York and London: Spon Press.

KRAHN, J., LAM, L. & NEWMAN, L. 2004. *Stability Modeling with SLOPE/W. An Engineering Methodology,* Calgary, GEO-SLOPE/W Internationa Ltd.

MARRA, V. 2013. On Solvers: Multigrid Methods. *COMSOL Blog* [Online]. Available from: http://www.comsol.com/blogs/on-solvers-multigrid-methods/ 2015].

MULTI-PHYSICS, C. 2015. Documentation. Stockholm.

NADIM, F., PEDERSEN, S. A. S., SCHIMIDT-THOMÉ, P., SIGMUNDSSON, F. & ENGDAHL, M. 2008. Natural Hazards in Nordic Countries. *Episodes,* 31**,** 176-184.

NIAN, T. K., CHEN, G. Q., WAN, S. S. & LUAN, M. T. 2011. Non-convergence Criterion on Slope Stability FE Analysis by Strength Reduction Method. *Journal of Convergence Information Technology,* 6**,** 78-88.

NORDAL, S. 2008. *Lecture notes: PhD Course BA8304. SOIL MODELLING,* Trondheim, Norwegian University of Science and Technology. Geotechnical Division.

NORDAL, S. 2011. *TBA4116 GEOTECHNICAL ENGINEERING, ADVANCED COURSE. Lecture notes and background material,* Trondheim, Norwegian University of Science and Technology. Geotechnical Division.

OLSSON, M. 2013. *On Rtae-Dependency of Gothenburg Clay.* Doctor of Philosophy, Chalmers University of Technology.

SLOVENIAN, E. C.-F. O. C. A. G. E. I. 2010. *ESDEP Course-Lecture 7.8.2: Restrained Beams II* [Online]. Available: http://www.fgg.uni-lj.si/~/pmoze/ESDEP/master/wg07/l0820.htm 20152015-05-21].

WOOD, D. M. 1990a. Chapter 1 Introduction: models and soil mechanics. *Soil behaviour and Critical State Soil Mechanics.* Cambridge: Press Syndicate of the University of Cambridge.

WOOD, D. M. 1990b. Chapter 2 Elasticity. *Soil behaviour and Critical State Soil Mechanics.* Cambridge: Press Syndicate of the University of Cambridge.

WOOD, D. M. 1990c. Chapter 3 Plasticity and Yielding. *Soil behaviour and Critical State Soil Mechanics.* Cambridge: Press Syndicate of the University of Cambridge.

WOOD, D. M. 1990d. Chapter 10 Stress paths and soil tests. *Soil behaviour and Critical State Soil Mechanics.* Cambridge: The Press Syndicate of the University of Cambridge.

WOOD, D. M. 2009. *Soil mechanics: a one-dimensional introduction,* Cambridge, Cambridge UniversityPress.

XU, G. L., HUANG, H., BAI, Y. S. & ZHANG, W. S. 2011. On the Application of Finite Element Method (FEM) to the Slope Stability Analyses. *Applied Mechanics and Materials,* 66-68**,** 1913.

Y . M . CHENG & LAU, C. K. 2014. Basic slope stability analysis methods. *Slope Stability Analysis and Stabilization.* CRC Press.

YU, H.-S. 2006. *Plasticity and Geotechnics*, Springer US.

ZHENG, H., LIU, D. F. & LI, C. G. 2005. Slope stability analysis based on elasto-plastic finite element method. *International Journal for Numerical Methods in Engineering,* 64**,** 1871-1888.

ZHENG, H., SUN, G. & LIU, D. 2009. A practical procedure for searching critical slip surfaces of slopes based on the strength reduction technique. *Computers and Geotechnics,* 36**,** 1-5.

APPENDIX A: Slip surfaces in PLAXIS and the selected stress points within failure zone for case 1.

Case 1: selection of 10 stress points in a coarse mesh

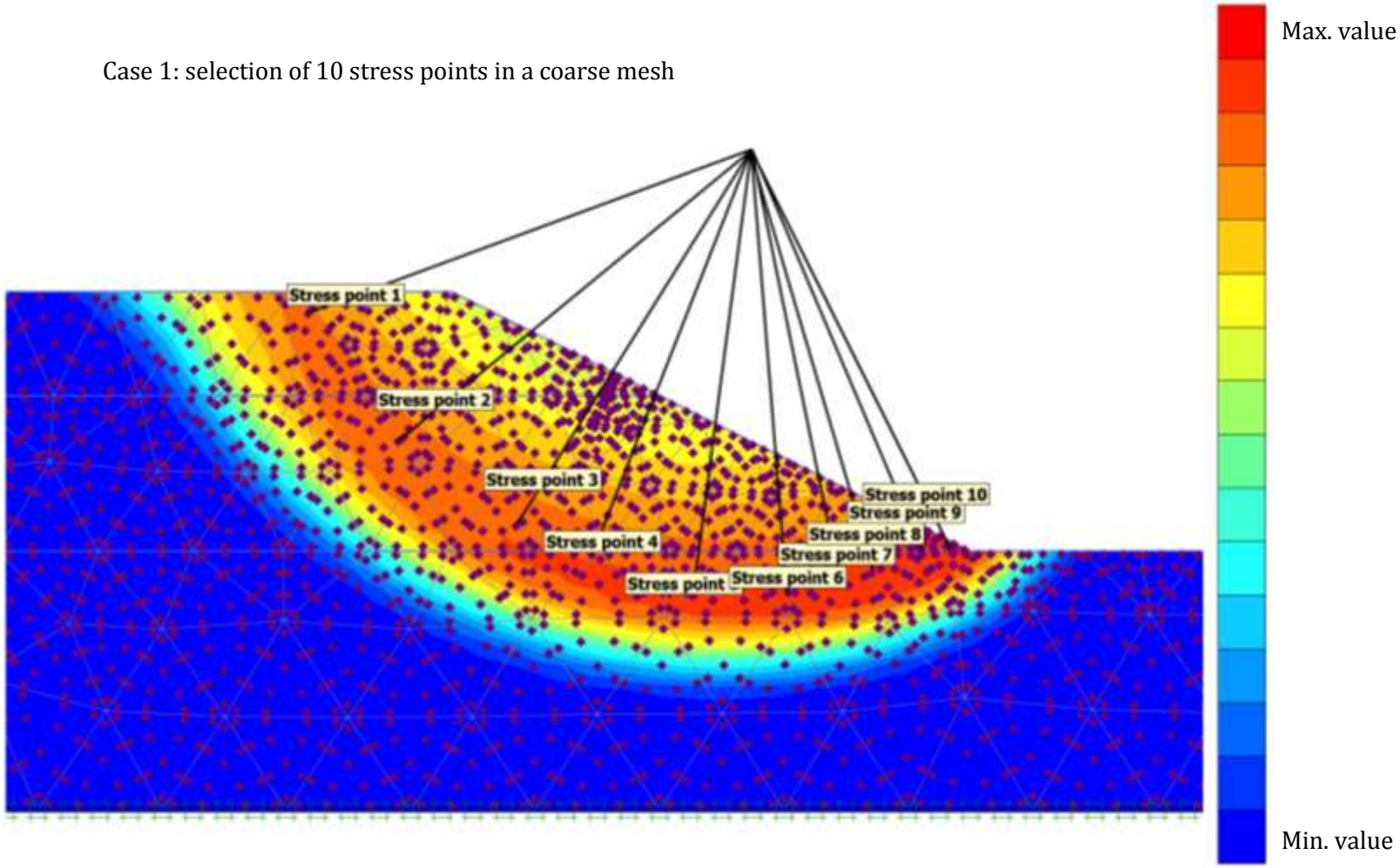

Figure 22. Slip surface and 10 selected points for case 1 with a coarse mesh

APPENDIX B: Slip surface in PLAXIS and the selected stress points along the failure zone for case 1 with a finer mesh

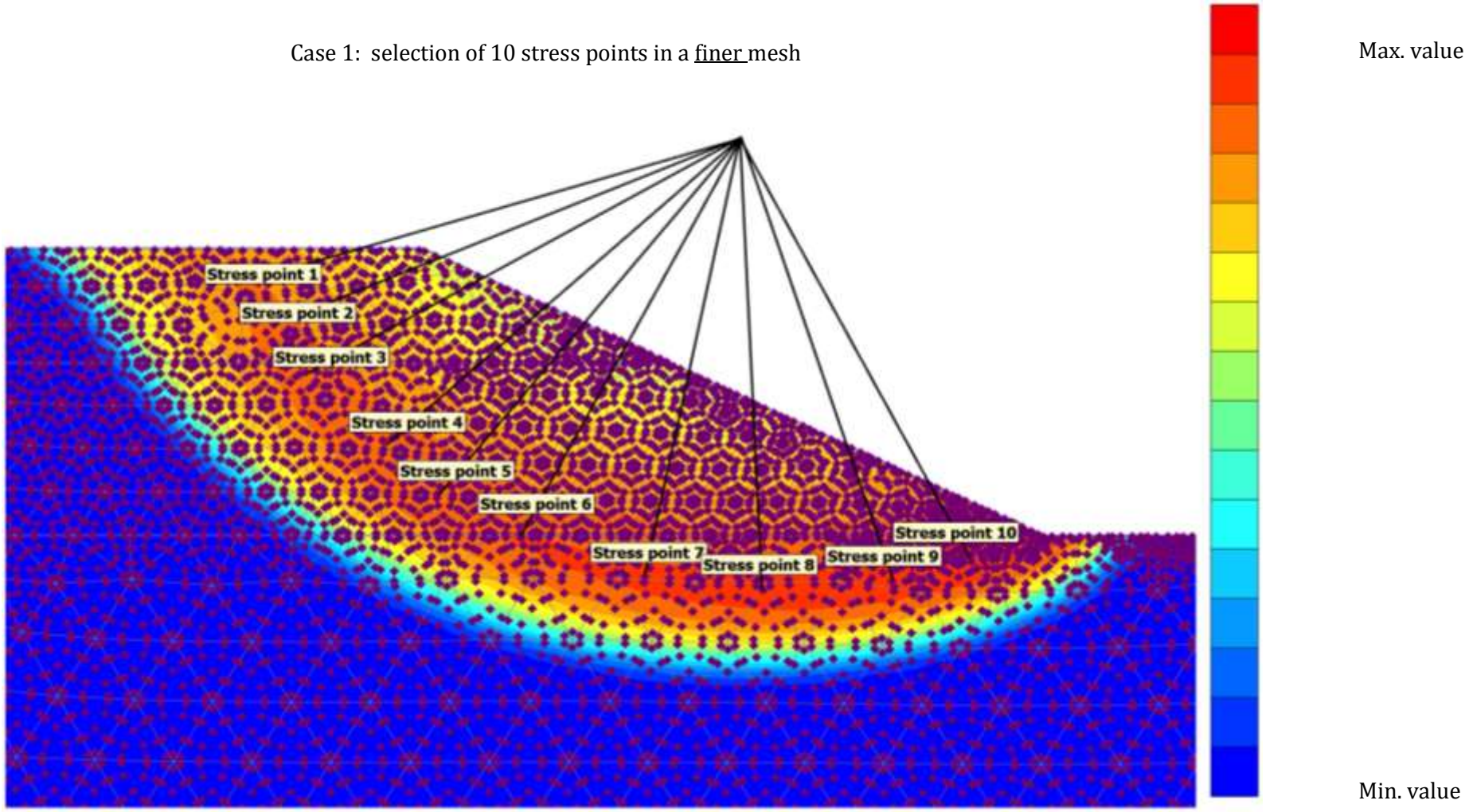

Figure 23. Slip surface and 10 selected points for case 1 with a finer mesh

APPENDIX C: Slip surface in PLAXIS and the selected stress points along the failure zone for case 2 (effective stresses).

Case 2: selection of 10 stress points in a coarse mesh

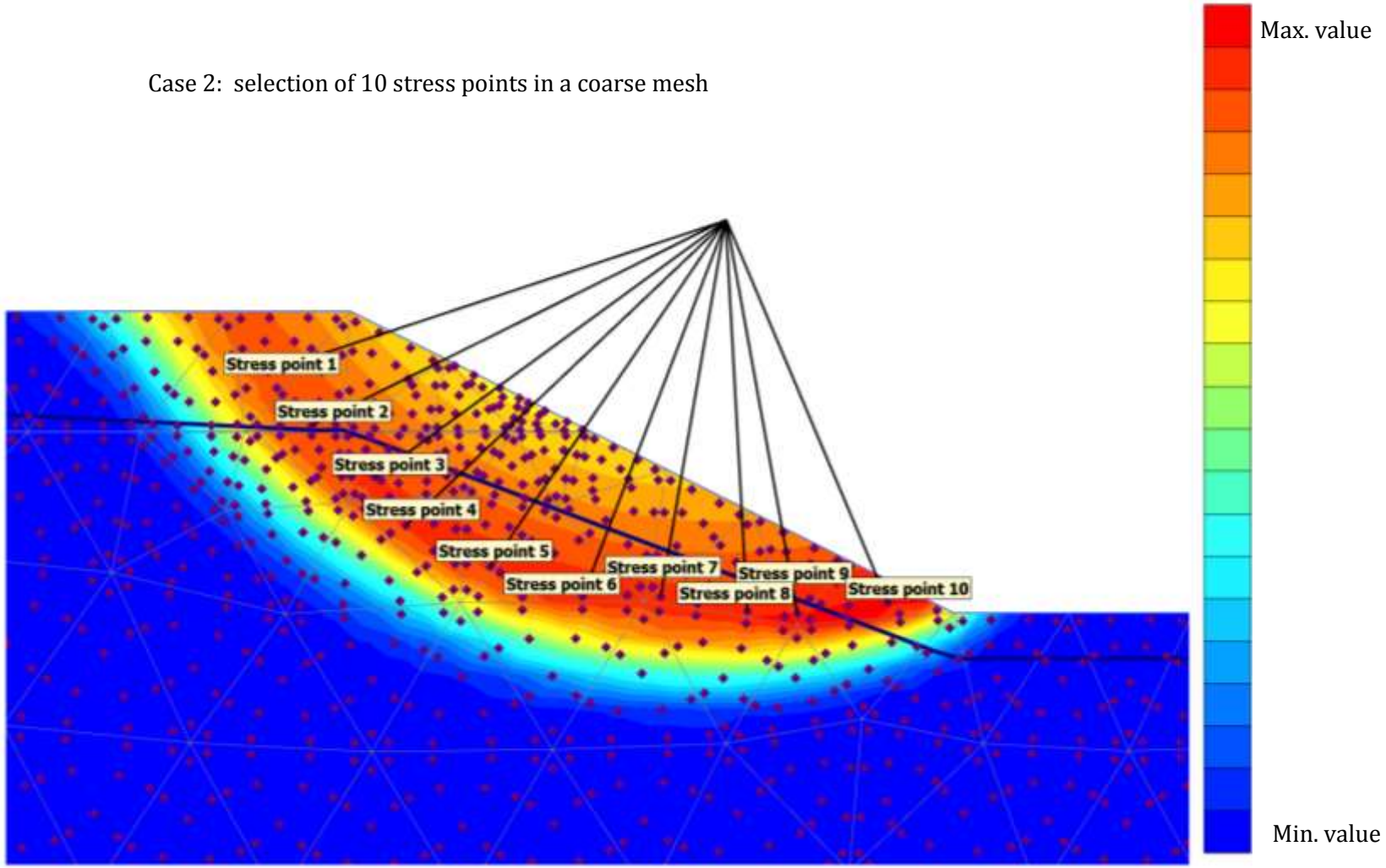

Figure 24. Slip surface and 10 selected points for case 2

APPENDIX D: Summary of parameters and mesh adjustments for case 1

Table 4. Soil parameters and mesh information for the tested options in case 2

Condition	Cu kPa	ϕ	ν	Mesh density	Average element size (PLAXIS) [m]	Element size parameters (COMSOL) [m]		No of elements	Nr. Nodes	DOF	Program	FOS	Difference	
						Max. size	min. size						FEM-FEM	FEM-LEM
total stress	20+2*Z	0	0.4	coarse	1.5750			242	2077		PLAXIS	2.106	2.06%	2.93%
total stress	20+2*Z	0	0.4	coarse		2.2200	0.0180	248		4226	COMSOL	2.149		5.05%
total stress	20+2*Z	0	NA	NA							SLOPE/W	2.046		
total stress	20+2*Z	0	0.4	fine	0.8462			838	6973		PLAXIS	2.103	1.83%	
total stress	20+2*Z	0	0.4	fine		1.0700	0.0180	993		16406	COMSOL	2.142		

APPENDIX E: Summary of parameters and mesh adjustments for case 2

Table 5. Soil parameters and mesh elements information for the tested options in case 2

Condition	Cu kPa	ϕ	ν	Mesh density	Average element size (PLAXIS)[m]	Element size parameters (COMSOL) [m]		No elements	No. Nodes	DOF	Program	FOS	Difference
						max. size	min. size						
effective densities	2	30	0.4	coarse	1.4010			382	3213		PLAXIS	1.580	2.53%
effective densities	2	30	0.4	coarse		3.0200	0.6000	260		4362	COMSOL	1.540	
effective densities	2	30	0.4	fine	0.3500			1359	11151		PLAXIS	1.545	2.27%
effective densities	2	30	0.4	fine		1.1500	0.6000	1333		21782	COMSOL	1.510	
effective densities	10	30	0.4	coarse	1.4010			382	3213		PLAXIS	2.730	2.56%
effective densities	10	30	0.4	coarse		3.0200	0.6000	260		4362	COMSOL	2.660	
effective densities	10	30	0.4	fine	0.7429			1413	11575		PLAXIS	2.705	2.03%
effective densities	10	30	0.4	fine		1.1500	0.6000	1333		21782	COMSOL	2.650	
effective stress	2	30	0.4	coarse	2.0580			177	1511		PLAXIS	1.361	5.66%
effective stress	2	30	0.4	coarse		3.0200	0.6000	260		4362	COMSOL	1.284	
effective stress	2	30	0.4	fine	0.7286			1413	11575		PLAXIS	1.316	NA
effective stress	2	30	0.4	fine		1.1500	0.6000	1333		21782	COMSOL	NA	
effective stress	10	30	0.4	coarse	2.0580			177	1511		PLAXIS	2.079	3.27%
effective stress	10	30	0.4	coarse		3.0200	0.6000	260		4362	COMSOL	2.011	
effective stress	10	30	0.4	fine	0.7041			1513	12387		PLAXIS	2.071	3.24%
effective stress	10	30	0.4	fine		1.0500	0.6000	1534		25034	COMSOL	2.004	

APPENDIX F: Different stress paths *s':t* curves for selected points in case 2: effective stress based analysis

In the following graphs, Figure 25- Figure 34, it is possible to observe closely the behaviour of the stress points. It is shown that in general curves have a similar shape and the starting points, indicated by a circle for PLAXIS and a square for COMSOL, are very alike. The horizontal and vertical scale is slightly different from graph to graph since it is adapted to show closely each curve.

It is possible to observe the slight difference in the resulting values which, as explained in the text, is thought to be related to the differences between both programs, mainly the interpolation process to obtain information in the domain probe points in COMSOL, as well as the meshing process and solver settings used.

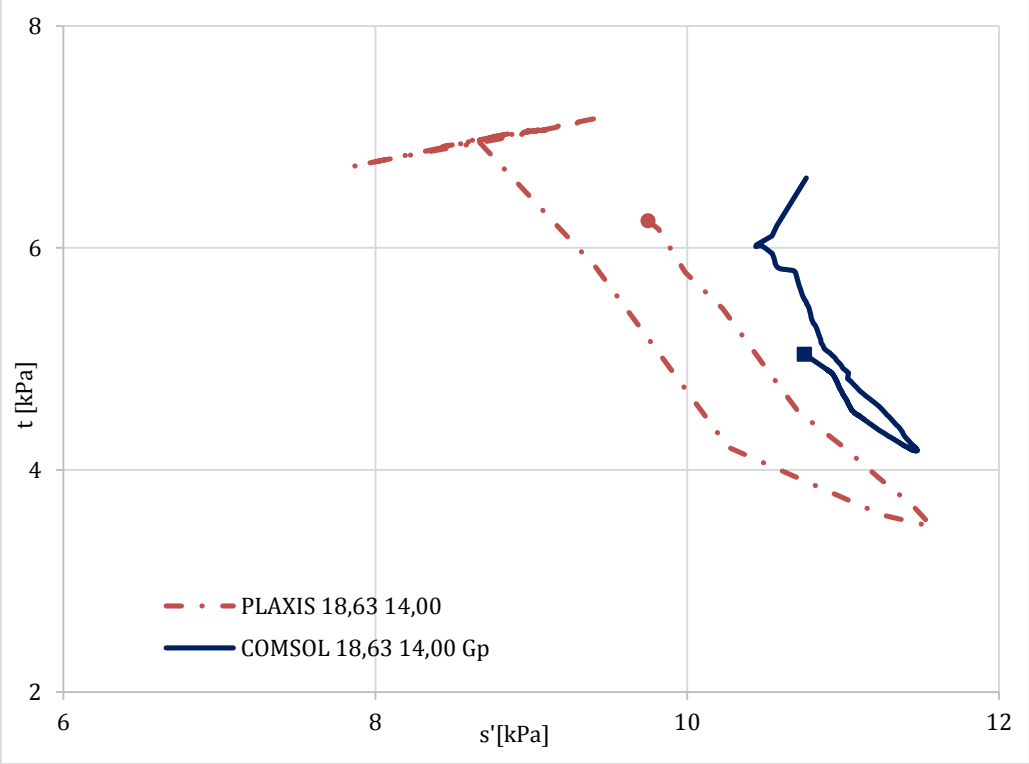

Figure 25. s':t curves for the selected point 1 (18,63 14,00) from Case 2 effective stress analysis

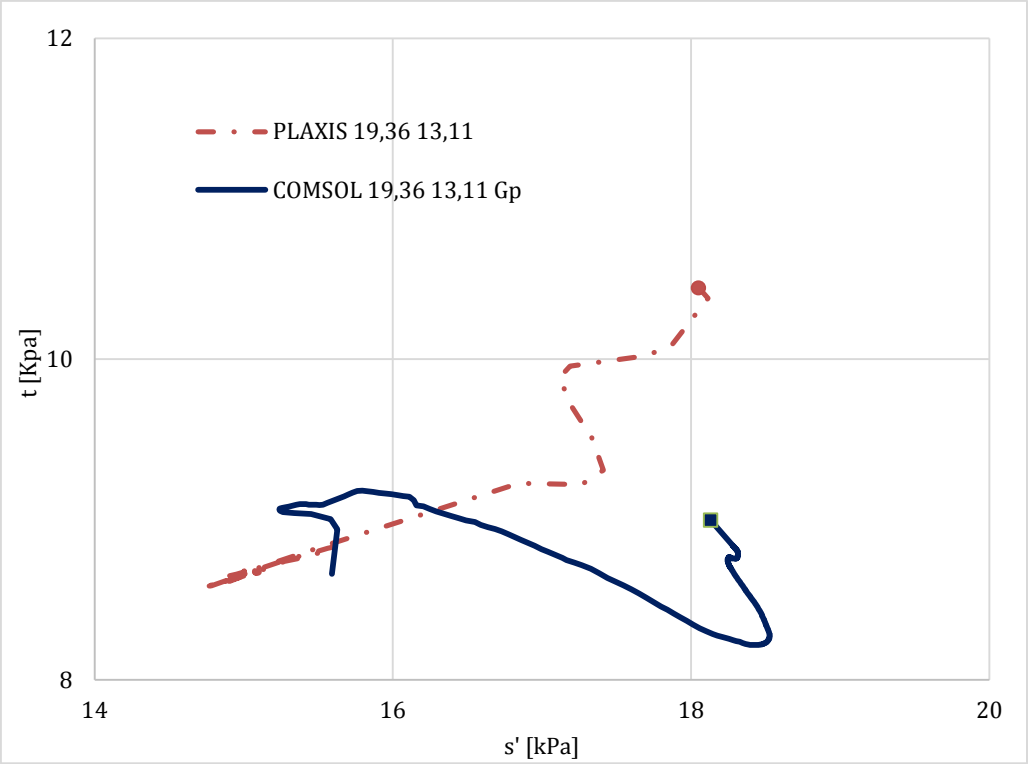

Figure 26. s':t curves for the selected point 2 (19,36 13,11) from Case 2 effective stress analysis

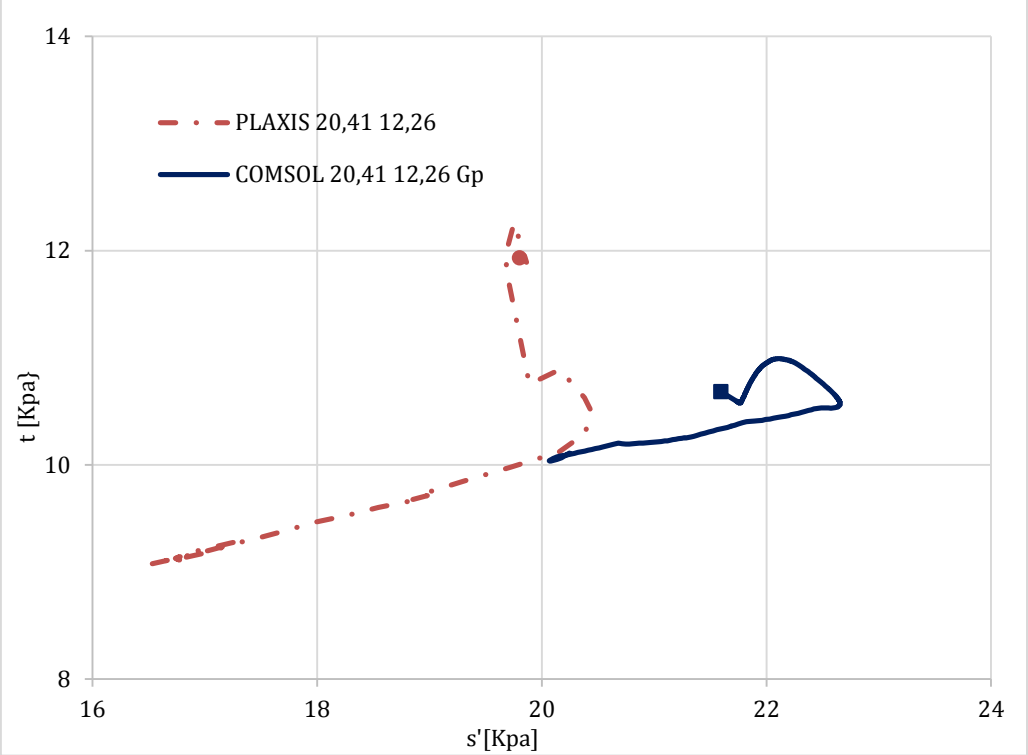

Figure 27. s':t curves for the selected point 3 (20,41 12,26) from Case 2 effective stress analysis

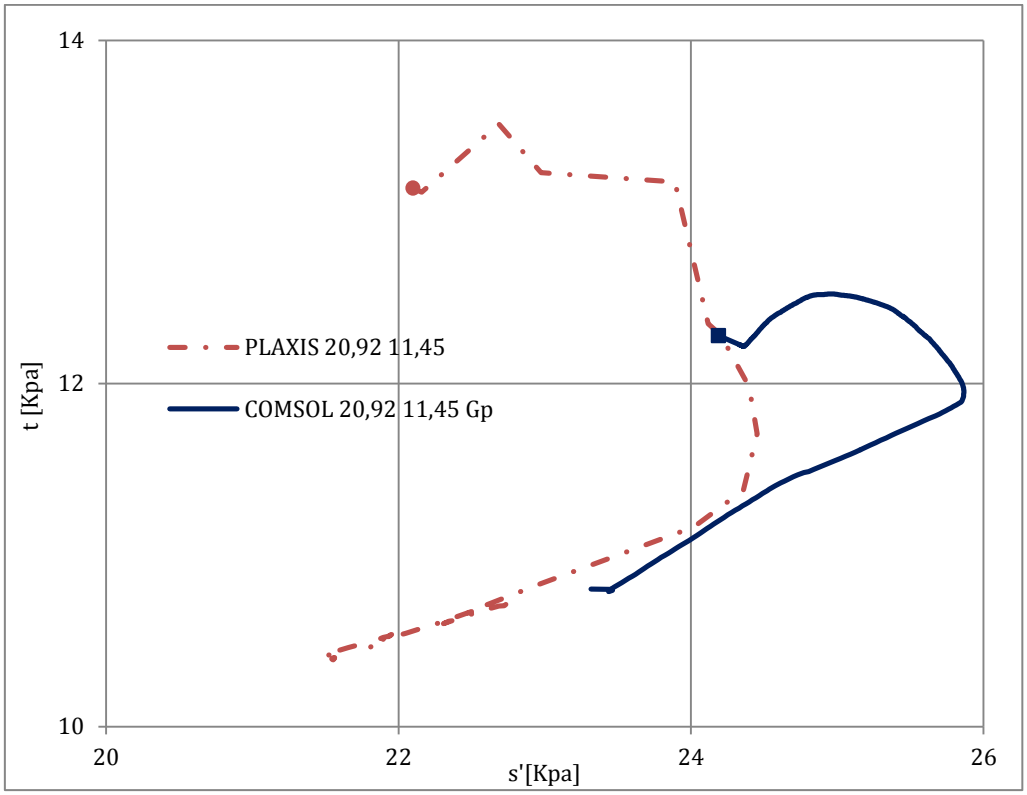

Figure 28. s':t curves for the selected point 4 (20,92 11,45) from Case 2 effective stress analysis

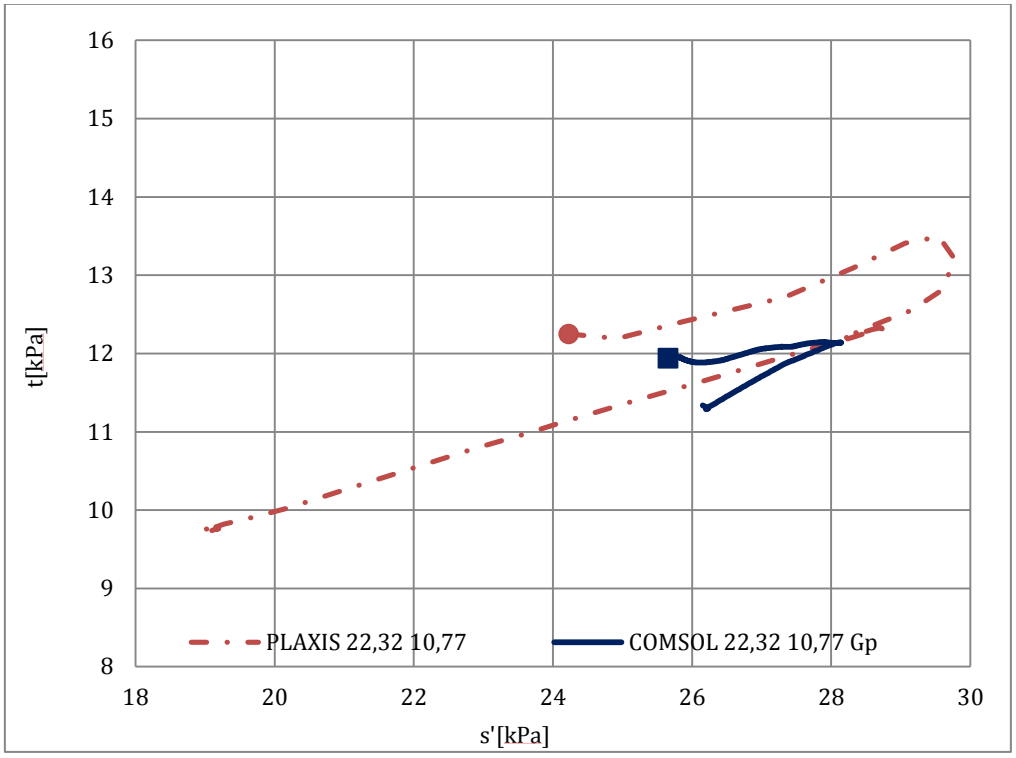

Figure 29. s':t curves for the selected point 5 (22,32 10,77) from Case 2 effective stress analysis

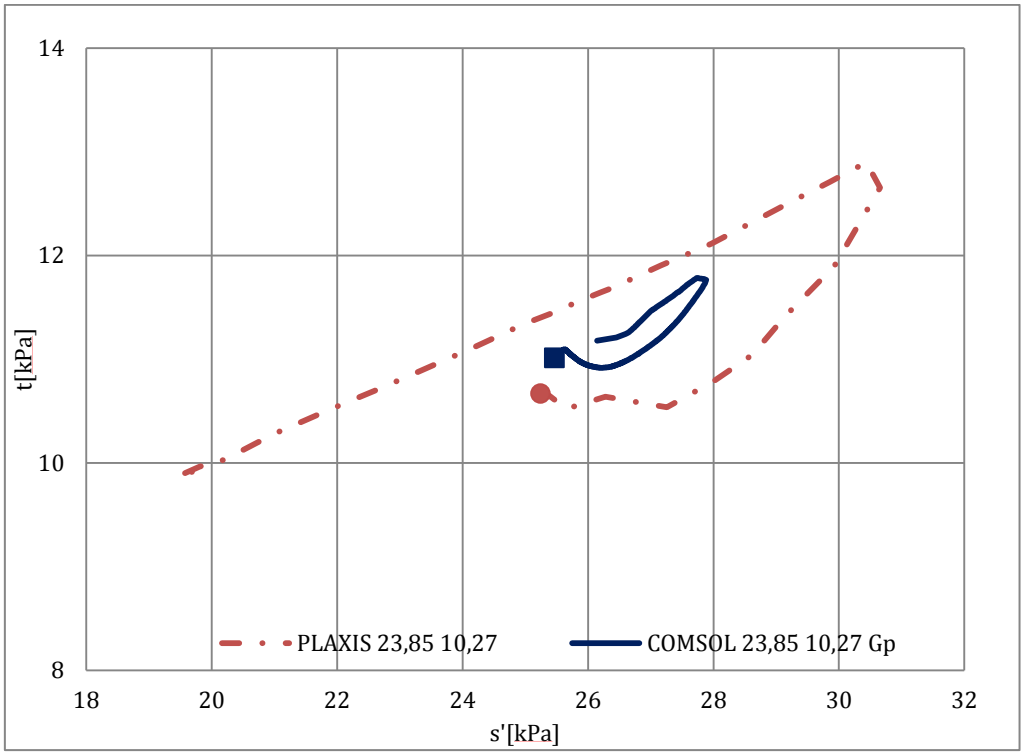

Figure 30. s':t curves for the selected point 6(23,85 10,27) from Case 2 effective stress analysis

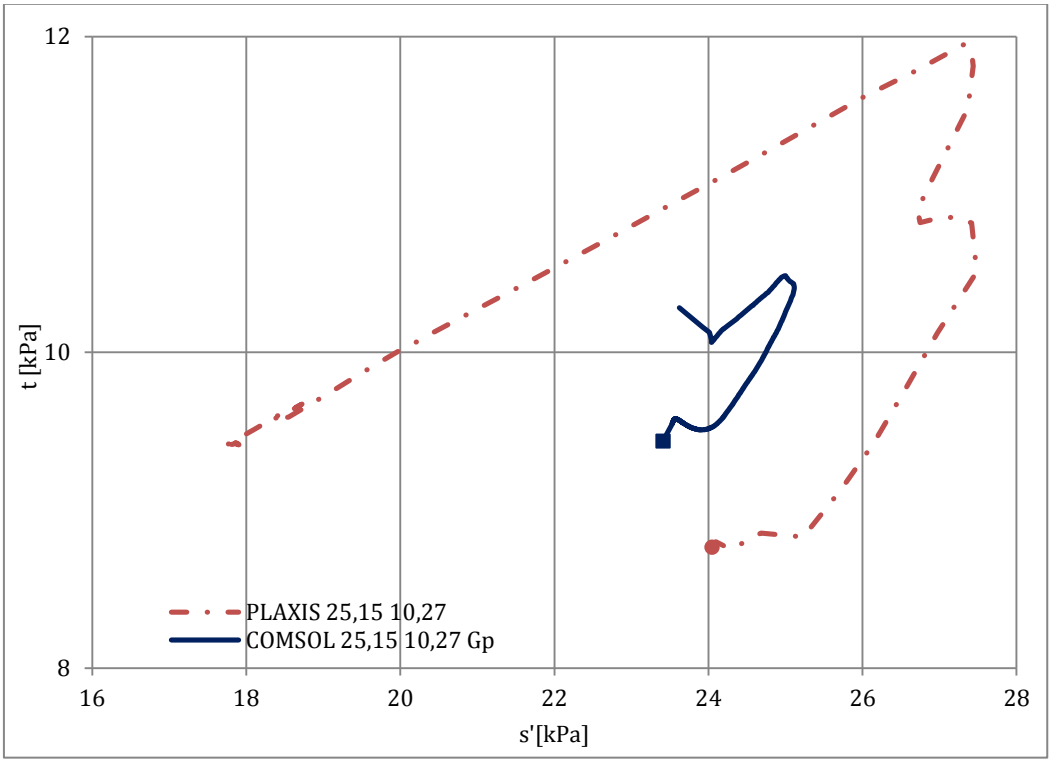

Figure 31. s':t curves for the selected point 7 (25,15 10,27) from Case 2 effective stress analysis

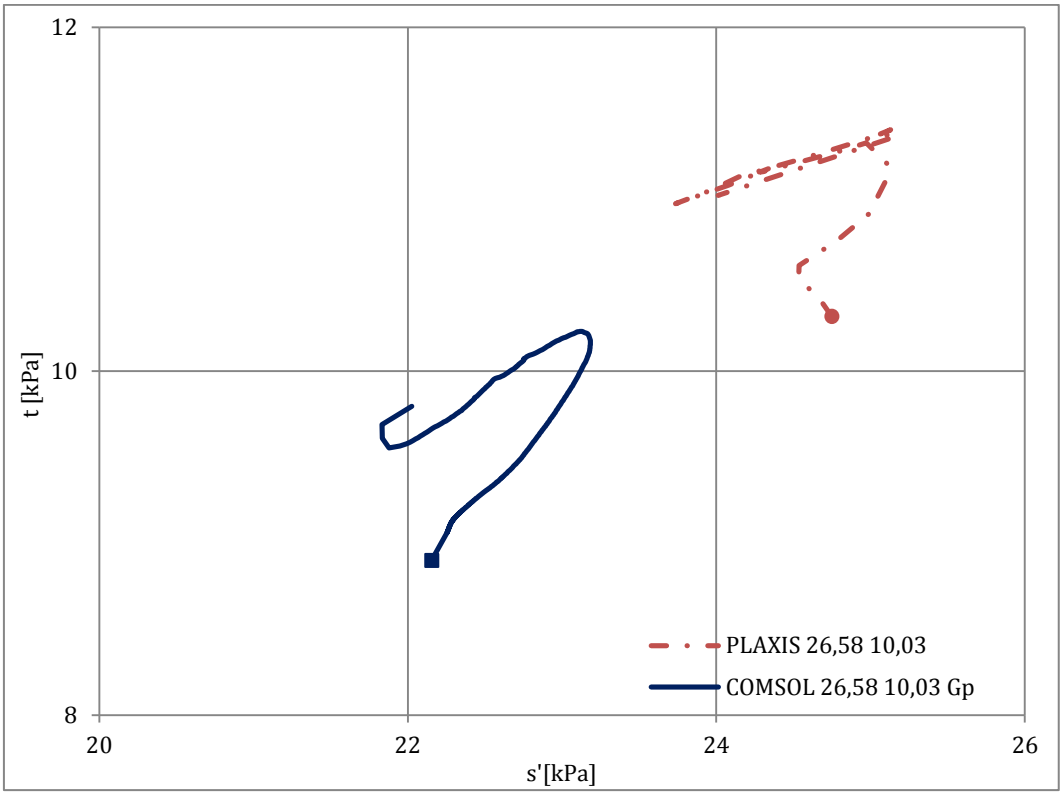

Figure 32. s':t curves for the selected point 8 (26,58 10,03) from Case 2 effective stress analysis

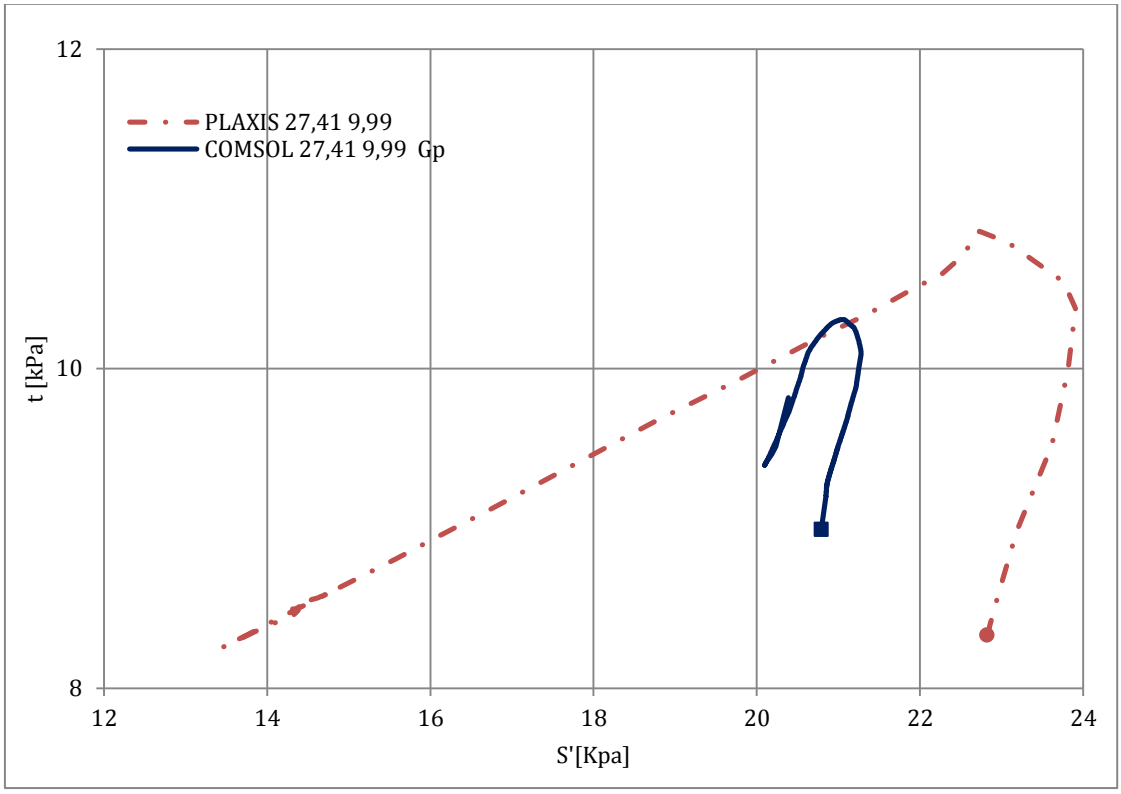

Figure 33. s':t curves for the selected point 9 (27,41 9,99) from Case 2 effective stress analysis

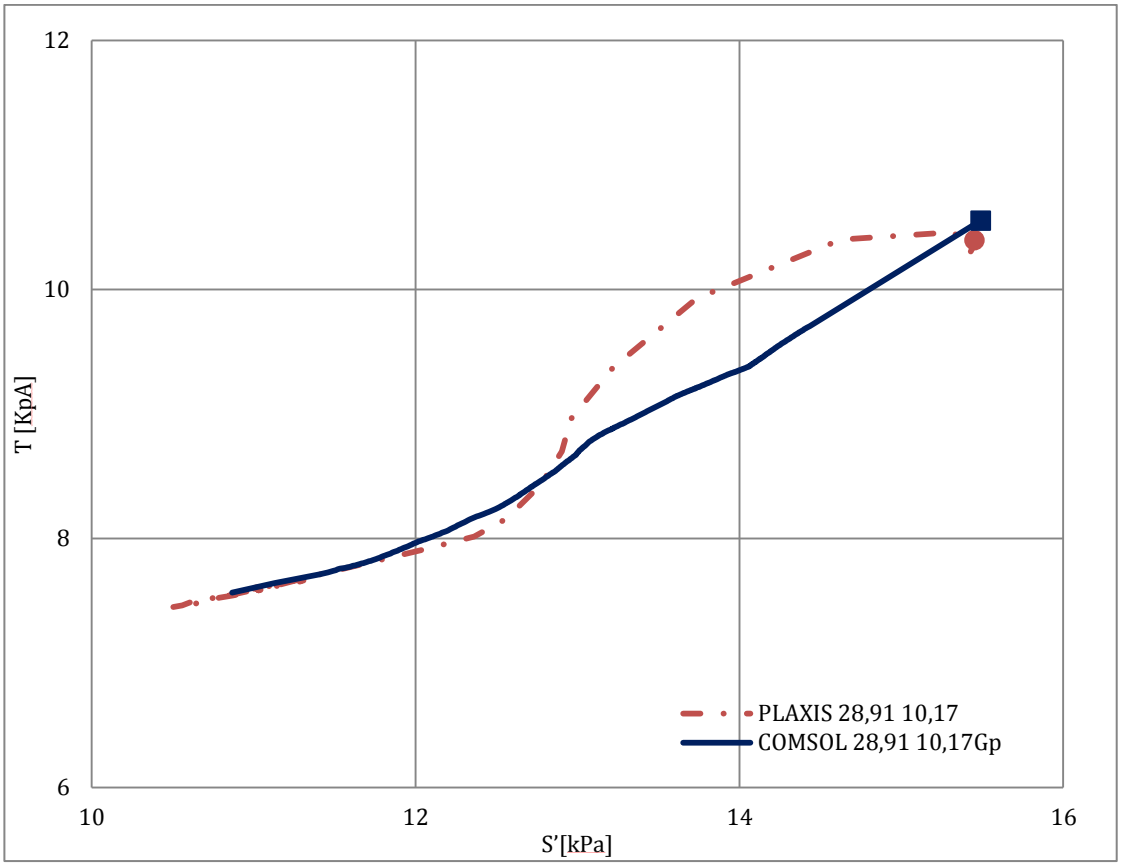

Figure 34. s':t curves for the selected point 10 (28,91 10,17) from Case 2 effective stress analysis